Characterisation of surface pretreatments for aluminium-epoxy joints

TS Laas

orcid.org/ 0000-0002-1962-9197

Dissertation accepted in fulfilment of the requirements for the degree *Master of Engineering in Mechanical Engineering* at the North-West University

Supervisor: Prof AS Jonker

Co-supervisor: Mr JD Human

Graduation: November 2023

Contents

List of figures

List of tables

Preface and acknowledgements

I dedicate this dissertation to the following:

My Heavenly Father, who has led me throughout my academic career and my life and has given me the talent of intellect and reasoning.

“For I know the plans I have for you, declares the Lord, plans to prosper you and not harm you, plans to give you hope and a future” – Jeremiah 29:11

My loving wife Dienkie, who has stood by my side throughout this study and supported me in every step. Thank you for being my best friend and supporter.

Prof. Attie Jonker for his guidance and thoughts and for embodying the role of a true study leader. Thank you for believing in my abilities and for trusting me with such an excellent study subject.

Mr Danie Human for his practical wisdom and for also granting me the opportunity for working on the NWU solar car. It was a true pleasure working alongside you.

Mr Sarel Naude for his help with the practical as well as the testing side of my study.

Dr Anine Jordaan for doing the SEM imaging seen in this study and for providing wisdom on how to interpret the resulting images.

Lastly, my family and friends who made the person I am today, one who could complete this master’s degree. Thank you for your constant love and support.

I am forever indebted to all who made this study possible, for it was not I who completed it, but all of us.

Abstract

This study investigated a modified phosphoric acid anodising (PAA) process and grit blasting as surface pretreatments to increase the strength and integrity of aluminium bonded with SpaBond 345 epoxy by Gurit. SpaBond 345 as an adhesive for aluminium is not widely documented but was shown in this study to have a high bond strength and durability.

Anodising and grit blasting have historically been used to successfully increase the strength of aluminium bonded with epoxy. Anodising is an electrochemical process that creates micropores on non-ferrous metal surfaces such as aluminium. Grit blasting mechanically cleans and prepares metal surfaces through a blasting medium, such as glass beads.

Testing was done based on the ASTM-D1002 standard, which uses single-lap joints to test the bonds' strength and durability. The overlap length of the joint was modified from 12.7 mm to 25 mm, to account for the difference in thickness of the aluminium used, while the crosshead speed was kept at 1.3 mm/minute per the standard. The single-lap joint samples were tested to failure in an MTS universal testing machine, and the maximum shear strengths were recorded. The testing conditions were unaged, 300 hours aged, and 600 hours aged in a 3% NaCl solution at 60 °C. Test results showed that anodising produced bonds that were on average stronger for all ageing conditions than grit blasted bonds.

After testing, all fractured samples were photographed, and a few were chosen for analysis by scanning electron microscope (SEM). The optical results showed cohesive and adhesive failure in the anodised samples, but only adhesive failure for the grit-blasted samples. Moisture ingress was more prevalent in the grit blasting samples than in the anodised samples, which is a deciding factor in the durability of a bond.

SEM analysis confirmed that the structures attained by PAA and grit blasting were consistent with what is found in the literature in terms of surface morphology and also how the epoxy was able to better adhere to the anodised samples even after ageing.

Anodising produced bonds with a higher lap shear strength in all ageing conditions and prevented moisture ingress to a greater extent than the grit-blasted joints. Grit-blasted joints are sufficient for non-critical applications to reduce costs, and anodising should be reserved for bonding critical components.

Keywords

Adhesion

Accelerated ageing

Aluminium

Anodising

Grit blasting

Lap shear testing

Scanning electron microscope

Single lap joints

SpaBond

1. Introduction

1.1. Background

During World War 2, the use of aluminium in aircraft construction became prevalent and eventually surpassed the use of wood. This was partly due to the declining costs of producing aluminium and partly because aircraft design necessitated materials with a high strength to weight ratio (Risbrudt *et al.*, 2007). Traditionally, riveting has been used to fasten aluminium panels and components on aircraft because they are low in cost and easy to install (Barrett, 1990). Rivets work by expanding into an interference fit in holes drilled into the aluminium components being fastened (Barrett, 1990). Laser beam welding (LBW) has also been used successfully to join aluminium components because it is lighter than rivets with up to 10% savings in panels on the A380 (Melhem, 2018). LBW also decreases the possibility of corrosion in the joints as well as fatigue cracking usually associated with riveting but increases the residual stresses around the weld (Melhem, 2018:37).

Over time, aircraft were increasingly built with aluminium and composite materials, and it was thus necessary to find a different method of bonding because riveting and welding these dissimilar materials were found to be unsuitable. Using rivets to join composites and aluminium requires both materials to be drilled which leads to the formation of stress concentrations (Legdin, 2017). Furthermore, Barrett (1990:29) states that solid rivets, most used in aircraft construction, expand into an interference fit and thus should not be used with composite materials as they may cause the composite to delaminate. Figure 1 clearly shows the difference in stress distributions of riveted and bonded joints (da Silva *et al.*, 2018).

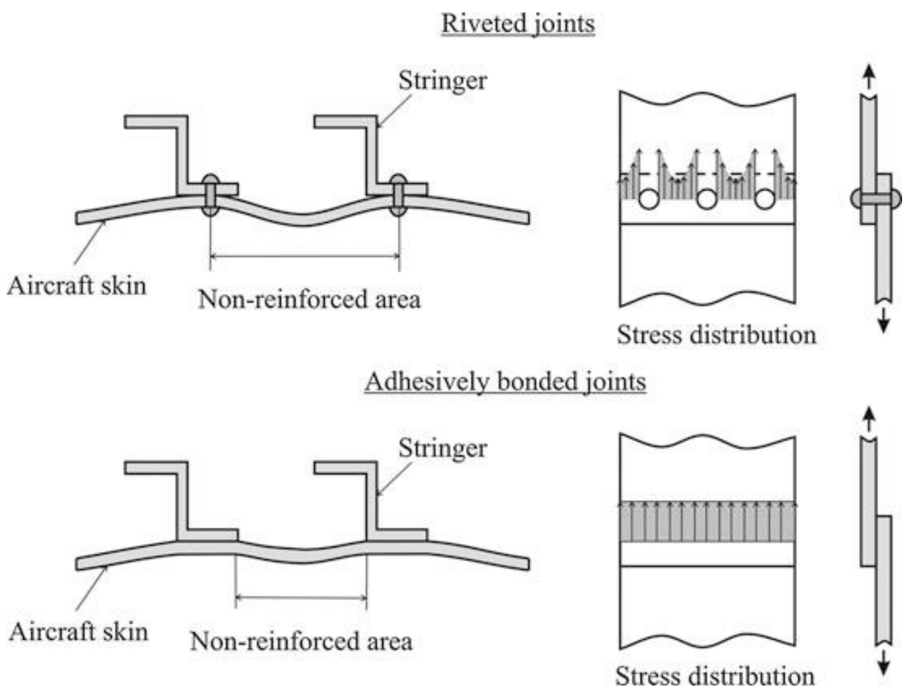

Figure 1: Improved stiffness and stress distribution in adhesively bonded joints (da Silva et al., 2018:3)

Legdin (2017:7-21) also notes galvanic corrosion as a further risk to riveting composites and aluminium. Laser welding has also been shown to be effective at joining fibre composite materials to aluminium (Zhang *et al.*, 2017). The adhesion of carbon fibre-reinforced polymer (CFRP) to epoxy is well-documented and only requires a simple treatment such as grit blasting or abrasion (Sorrentino *et al.*, 2018); hence, it is not the focus of this study.

Adhesives such as epoxies and tapes have become ever more popular as a method of fastening aluminium to itself or dissimilar materials. Most epoxies and tapes will adhere to any surface, but strong and durable adhesive bonds are created only when the surfaces being bonded are free from contaminants, such as oils, and have an appropriate micro and macro structure for the adhesive being applied (da Silva *et al.*, 2018). This surface needs to have the correct surface energy and morphology to allow for adsorption or mechanical interlocking to keep the bonded surfaces together (da Silva *et al.*, 2006). These epoxies have various advantages over rivets including improved stress distributions at bonding area and no risk of galvanic corrosion (Legdin, 2017). An example of such an epoxy, SpaBond 345, is a toughened thixotropic paste that has great gap filling properties. It has been used to adhere steel and CFRPs, but no literature could be found that documents its usage with aluminium adherends (Borrie *et al.*, 2021).

Aluminium naturally forms a relatively smooth and thin oxide layer on its surface, and the structure of this layer is not conducive to adhesion due to low surface energies and surface roughness, which is why surface pretreatments are necessary prior to bonding (da Silva *et al.*, 2018:1317). Momm *et al*. (2021) note various examples of debonding on aircraft that led to damage to the aircraft and in some cases even harm or death to occupants. One of the most famous incidents involved an Aloha Airlines Boeing 737 that lost part of its fuselage due to bond failure and fatigue cracks along the rivet holes (Board, 1989). This incident led to one fatality and various occupant injuries and highlights not only the importance of a properly pretreated bond surface, but also the stresses caused by riveting. In 1999 a glider’s wing broke off and led to the destruction of the aircraft. The investigation found that bond failure between aluminium and composite fibre components on the aircraft to be a major contributing factor to the incident (Demko *et al.*, 1999)

One of the first aluminium surface pretreatments used was a simple acid etch developed by Forest Products Laboratory (FPL), which would later be known as the FPL etch (Risbrudt *et al.*, 2007). Further research led to chromic acid anodising (CAA), an electrochemical pretreatment that produced strong and durable bonds (Critchlow & Brewis, 1996). Both processes used various forms of chromic acid, which in some instances contain hexavalent chromium, a highly carcinogenic substance that is harmful to the environment (Labor, 2006). A transition was made to cleaner and safer alternatives in recent years; these include the P2 etch, phosphoric acid anodising (PAA), laser engraving, and grit blasting (Critchlow *et al.*, 2006).

The decision to choose a pretreatment is further motivated by cost, complexity, and time consumption. Anodising is generally costly and complex to establish in an industrial environment due to the high cost of energy usage, chemical procurement, and disposal and infrastructure development (da Silva *et al.*, 2018:149-150) Grit blasting is generally considered more cost effective and simpler to implement, but does not have the same bond strength and durability of anodising (Critchlow & Brewis, 1996).

1.2. Problem statement

The shear strength and bond durability of aluminium bonded with epoxy, using grit blasting versus phosphoric acid anodising as a surface preparation method requires investigation to confirm the differences in these parameters between treatments. Furthermore, no data in the literature is available on the bond strength and durability between SpaBond 345 and pretreated aluminium.

1.3. Methodology

A literature study will be performed to further identify and analyse the problem and consider possible solutions. An experimental procedure will be developed to anodise, and grit blast the aluminium samples. Testing will be done to failure according to a modified ASTM-D1002 standard. The empirical data obtained through experimentation will be used to investigate the issues identified in the problem statement. Visual and SEM analysis will be done on the treated and fractured surfaces. Conclusions will be made from the collected data as it might apply to the study, and suggestions for further study will be made.

1.4. Chapter layout

Chapter 2 contains the literature study of research that has been done in the field of anodising and adhesion, as well as the methods of testing and analysis of bonded joints. Chapter 3 outlines and describes the experimental procedures and the materials used. The results and discussion are given in Chapter 4. Conclusions are given in Chapter 5, and recommendations for future work in Chapter 6.

2. Literature Review

This section discusses aluminium bonding in terms of adhesion theory, surface pretreatments, accelerated ageing, and bonding testing methods.

2.1. Adhesion theory

The adsorption and mechanical theories of adhesion are the primary driving forces for the bonding of aluminium and epoxy. The Handbook of Adhesion Technology states that "[t]he essential idea of the adsorption theory of adhesion is that whenever there is contact between two materials at a molecular level, there will be adhesion" (da Silva *et al.*, 2018:16). Da Silva *et al.* (2018:18) further note that these attractive forces are primarily dispersion forces. The effectiveness of these forces between two materials is increased when the surface of the adherend is free from contaminants and is modified to provide structures, such as micro fibrous tendrils produced by PAA, that will decrease the intermolecular range to the adhesive (da Silva *et al.*, 2018). In Figure 2, the intermolecular forces between the adherend, and adhesive are represented by the dashed red lines.

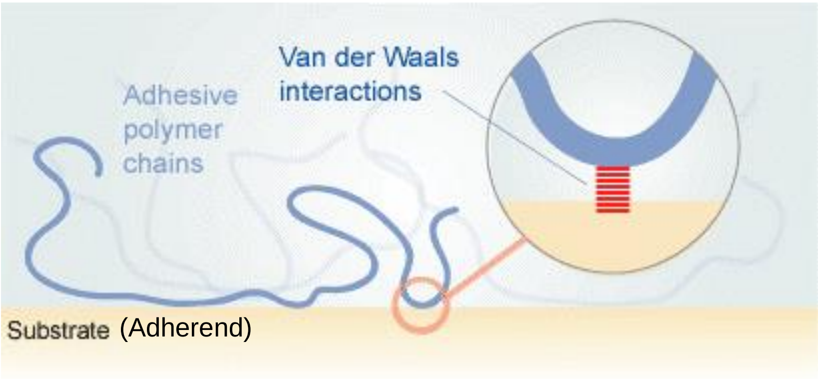

Figure 2: Modified schematic of adsorption theory (Mattson).

The mechanical theory emphasises that interlocking between the adhesive and adherend surface is necessary for proper adhesion (da Silva *et al.*, 2018:21). The primary method of increasing mechanical interlocking is by roughening up the surface of the adherend on a micro- and macro-scale whilst also keeping it free of contaminants (da Silva *et al.*, 2018). This roughening creates pores and crevices for the epoxy to run into (da Silva *et al.*, 2018). Figure 3 shows the mechanical interlocking that is possible between an adherend and adhesive.

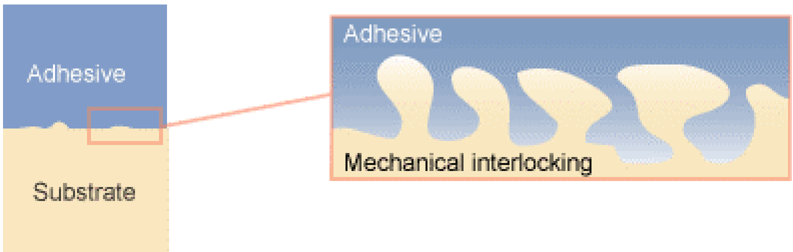

Figure 3: Schematic of mechanical interlocking (Mattson).

These theories are closely connected and share two common concepts: wettability and surface energy. Wettability describes the tendency of a liquid to spread out over a surface (da Silva *et al.*, 2018). In view of adsorption, the more an epoxy can wet a surface, the more surface area there is for the dispersive forces to act upon, increasing the bond strength (da Silva *et al.*, 2018). Similarly, if an epoxy can thoroughly wet a rough surface, mechanical interlocking also increases (da Silva *et al.*, 2018). The wettability of a surface can be predicted by considering its surface energy relative to that of the liquid being spread over it (Xu *et al.*, 2016). The greater the difference in surface energy between the two materials, the greater the attractive forces (da Silva *et al.*, 2018).

The surface energy of aluminium in its natural state has a low surface energy of between 24-45 mJ/m^2 (Kang & Choi, 2021; Matta *et al.*, 2022; Narbon *et al.*, 2018; Ostapiuk *et al.*, 2014; Petersson *et al.*, 2011). Given that epoxies, on average, have a surface energy of 45 mJ/m^2, it is necessary to apply a pretreatment to aluminium to increase its surface energy to between 69.8-75 mJ/m^2, and hence increase the wetting of the epoxy (Aspenes *et al.*, 2008; Coulon & Maillard, 2010; Higgins, 1988; K & Alagar, 2014; Li *et al.*, 2014; Rudawska *et al.*, 2017).

2.2. Aluminium pretreatments

Surface pretreatments are necessary to ensure proper adhesion between the surface of the aluminium and the adhesive being used (da Silva *et al.*, 2018). Aluminium is naturally resistive to adhesion because of the natural oxide layer on its surface that lowers its surface energy and, consequently, its wettability (da Silva *et al.*, 2018). Thus, it is necessary to use a pretreatment method that cleans off the natural oxide layer and creates a new, stable and ordered oxide layer with a surface morphology that promotes adhesion (Critchlow *et al.*, 2006). This structure is shown in Figure 4 after the CAA process. In addition, the surface energy of the aluminium needs to be higher than the epoxy to ensure adequate molecular contact with the adhesive (da Silva *et al.*, 2018:23). This means the introduction of micropits and even tendrils on the aluminium surface (Critchlow & Brewis, 1996). The following subsections consider some of the most common pretreatments used mainly in aerospace.

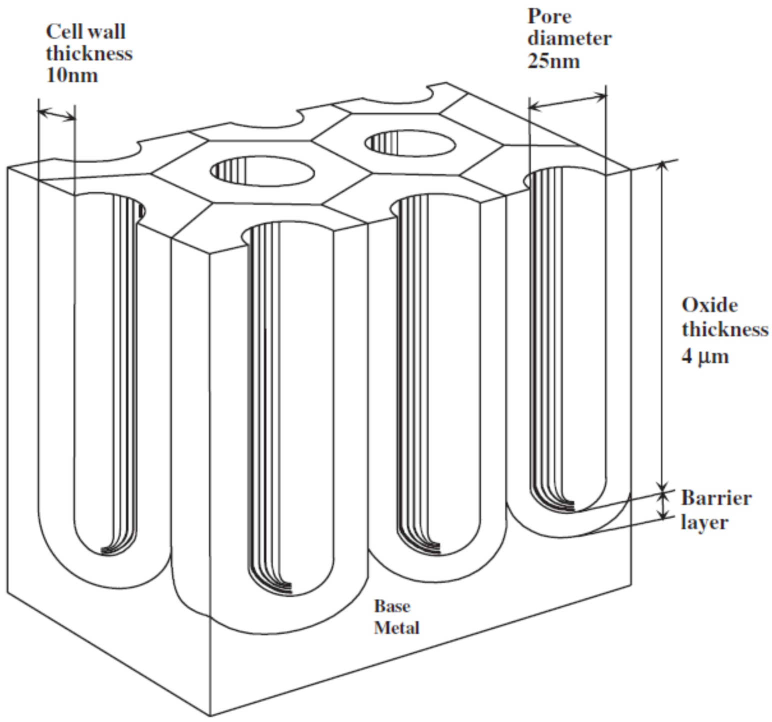

Figure 4: Idealised anodic oxide structure formed on clad alloys following the 40/50V CAA process (Critchlow et al., 2006)

2.2.1. Etching

Etching is a chemical pretreatment that involves using acids or alkalis to clean a metallic surface of contaminants, such as grease or oxides, and to create a micro-rough structure by dissolving the base metal (da Silva *et al.*, 2018:146). The FPL etching process is one of the oldest etching methods, which creates a micro-rough oxide layer on the surface of aluminium (Critchlow & Brewis, 1996:258; da Silva *et al.*, 2018:178). This process has been in use since the mid-1900s and saw its first use in World War 2, when the transition was made from wooden to aluminium aircraft (Risbrudt *et al.*, 2007). It consists of sodium dichromate (Na_2CrO_7) and sulphuric acid (H_2SO_4) in water (H_2O), with a process temperature of 68 °C for 10-30 minutes (da Silva *et al.*, 2018; Digby & Packham, 1995). It has been used in Boeing's BAC 5555 and despite its wide adoption and high adhesion strength, many manufacturers are seeking alternatives due to its use of hexavalent chromium, which is carcinogenic (Critchlow & Brewis, 1996; Critchlow *et al.*, 2006; Labor, 2006).

The P2 etch was developed as an alternative to the FPL etch (da Silva *et al.*, 2018:178; Digby & Packham, 1995). It creates a similar oxide layer morphology and adhesion strength as the FPL etch, without the use of toxic chromate components (Erich *et al.*, 2015; Ozenc & Sekercioglu, 2013). The process uses ferric sulphate ($FeSO_4$) and sulphuric acid (H_2SO_4) in water (H_2O) at 60-70 °C for 8-15 minutes (da Silva *et al.*, 2018; Digby & Packham, 1995).

A sodium hydroxide ($NaOH$) etch is very effective at dissolving the natural oxide layer on aluminium (Saleema *et al.*, 2012). Even though they can be used independently, P2 and NaOH etches are sometimes used together to prepare aluminium for anodising (da Silva *et al.*, 2018). This is because etching activates the aluminium surface and creates a clean surface for the new oxide layer to be formed by anodising (Prolongo

& Ureña, 2009).Sodium hydroxide etching has shown shear strengths of between 5MPa to 20MPa (Prolongo & Ureña, 2009; Saleema *et al.*, 2012)

2.2.2. Acid anodising

Anodising is an electrochemical pretreatment that uses an electrical circuit through an acidic electrolyte to modify the surface of non-ferrous metals, such as aluminium and titanium(da Silva *et al.*, 2018). The part to be anodised is positively charged and thus, it is the anode and is placed in an electrolyte bath along with a cathode, which can be made from a similar material as the anode. When current is passed through the circuit, the resulting electrochemical process accelerates oxidation on the surface of the metal part whilst also forcing the oxide layer to form in a controlled manner (Council; da Silva *et al.*, 2018; Kudelka, 2011). The resulting oxide layer that forms is controlled by varying the anodising process parameters such as voltage, current, acid concentration, and immersion time (Abd-Elnaiem *et al.*, 2019; Araoyinbo *et al.*, 2010).

The oxide layer can be characterised by several parameters, but emphasis is placed on the following qualitative and quantitative characteristics. Qualitative characteristics include corrosion resistance, surface lubricity and surface morphology, while quantitative characteristics include pore diameter, pore depth, pore wall thickness and layer thickness (da Silva *et al.*, 2018). Each of the quantitative characteristics have optimal values depending on the end use. Larger pore sizes lead to better mechanical interlocking but may decrease corrosion resistance; a thinner oxide layer is better suited for dimensionally accurate parts but may also decrease joint strength (Critchlow *et al.*, 2006; da Silva *et al.*, 2018). Figure 5 shows a schematic of an anodising bath with the cathodes on either side of the tank negatively charged and the anode, or workpiece, positively charged in the middle. The most popular methods for anodising aluminium include chromic acid anodising (CAA), boric sulfuric acid anodising (BSAA), sulfuric acid anodising (SAA) and phosphoric acid anodising (PAA) are discussed below.

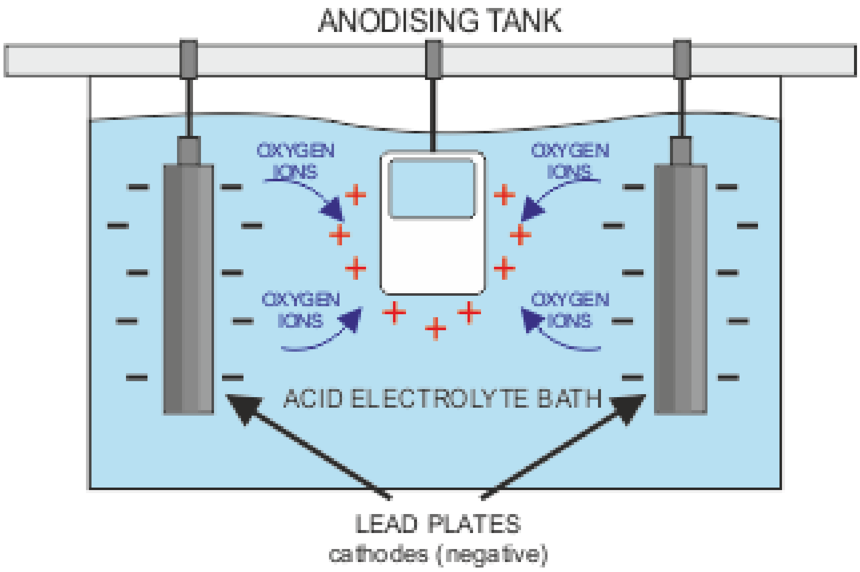

Figure 5: Schematic of anodising bath (Ryan, 2018).

CAA has for many years been one of the preferred methods for aluminium surface pretreatment in aircraft manufacturing (da Silva *et al.*, 2018). It is described in standards such as ASTM B580-79; MIL-A-8625 Type I, II, IIB, III; or MIL-C-60536, amongst others. It produces the thinnest oxide layer out of the three main types of anodising at between 0.001-0.005 mm (da Silva *et al.*, 2018). The pore sizes for the oxide layer can vary from 12-25 nm, with a wall thickness of 10 nm (Critchlow *et al.*, 2006; Ding *et al.*, 2018). It is considered a good option when tight tolerances on parts and superior bond strength are necessary. However, Ding *et al. (2018:32)* notes that "the CAA process uses a significant amount of chromic acid, which is a huge environmental liability for manufacturing, handling, and waste management". Critchlow *et al.* (2006:425) comes to the same conclusion when stating that "[t]his process utilises 40 gl^{-1} of hexavalent chromium which is hazardous to handle and operate and has large disposal costs".

BSAA was developed as an alternative to CAA (Critchlow *et al.*, 2006). It is more energy-efficient, cheaper, safer and more environmentally friendly (Critchlow *et al.*, 2006). It bears the same properties as CAA and, in some cases, even outperforms it with regards to corrosion resistance, paint adhesion and manufacturing practicality (Critchlow *et al.*, 2006). It is designated under standards such as Boeing's BAC 5632 and MIL-A-8625 (Corporation, 2015; PriceWalgren, 2020).

SAA also known as Type II anodising, is one the most-used method of anodising metals (da Silva *et al.*, 2018). It can produce a surface film with thicknesses in the range of 0.010mm, which is thicker than either CAA or PAA (da Silva *et al.*, 2018). The pore diameter of SAA ranges between 4.2 nm to 24 nm depending on the anodising voltage and temperature (Sulka & Parkola, 2006; Sulka & Parkola, 2007). The concern with SAA is that it does not provide the same joint strength or long-term durability of the joint when compared to CAA or PAA (Critchlow & Brewis, 1996). SAA is mostly applied to parts that require corrosion protection (da Silva *et al.*, 2018; PriceWalgren, 2020).

The Boeing Company developed PAA, which is classified under their BAC5555 process and is also defined by ASTM D3933 (Critchlow & Brewis, 1996; da Silva *et al.*, 2018). The typical oxide layer thickness is 400 nm, with 100 nm oxide tendrils protruding from the surface (da Silva *et al.*, 2018). As with other oxidation processes, the oxide layer is well structured with 10 nm thick cell walls separating pores with diameters of 30-900 nm, depending on anodising parameters (Cartwright, 2005; Lee *et al.*, 2016). PAA treated surfaces can withstand high humidity environments especially when bonded with epoxies (da Silva *et al.*, 2018). Tests show that surfaces prepared by PAA can withstand environmental stresses due to water immersion or salt spray testing and retain up to 85% of their original shear strength (Pires *et al.*, 2005).

A variety of PAA processes have been studied, with each study changing different aspects to observe the effects thereof. Xu *et al.* (2016) investigated the effects of differences in acid concentration, temperature, voltage and time of the anodisation process on the lap shear strength of aluminium samples. They noted that 130 g/l H_3PO_4 at 20 ˚C and 10 V for 20 min provided the higher lap shear strength at 52.45 MPa. PAA is usually combined with other pretreatments as part of a surface preparation regime. PAA in combination with alkaline etching and acid pickling have been shown to be effective at improving the lap shear strength retention, after ageing, of aluminium 2024-T3 samples by up to 10% (Pires *et al.*, 2005). Lee *et al.* (2016) varied H_3PO_4 temperature between 273 K and 313 K and voltage between 60V to 100V achieved bond strengths of between 17 MPa to 24.1 MPa. These studies have reported adhesive bond strengths of 17.0-52.45 MPa, depending on the anodisation parameters and the adhesive used (Ataberk, 2020; Digby & Packham, 1995; Lee *et al.*, 2016; Pires *et al.*, 2005; Xu *et al.*, 2016). A custom PAA process was created as the focus of this study and will be detailed in the experimental method section.

2.2.3. Grit blasting

Grit blasting is a mechanical pretreatment that works by accelerating small, abrasive particles, through a medium such as air or water, at a surface to clean it of contaminants and roughen it by abrasion (da Silva *et al.*, 2018). These abrasive particles can be in the range of 71 µm to 350 µm depending on the required surface morphology (Harris & Beevers, 1999; Slătineanu *et al.*, 2011).The most common use of grit blasting is the removal of rust from steel with sand as part of a restoration process. It has a low initial cost compared to other pretreatment methods such as anodising, but it creates bonds that are less durable and can produce inconsistent results due to the difficulty of controlling its working parameters (Critchlow & Brewis, 1996). Some of these parameters are the stand-off distance and impingement angle of the blasting nozzle from the workpiece, as shown in Figure 6, and the dwell time of the nozzle over a given section of the component (Cartwright, 2005; Romoli *et al.*, 2018).

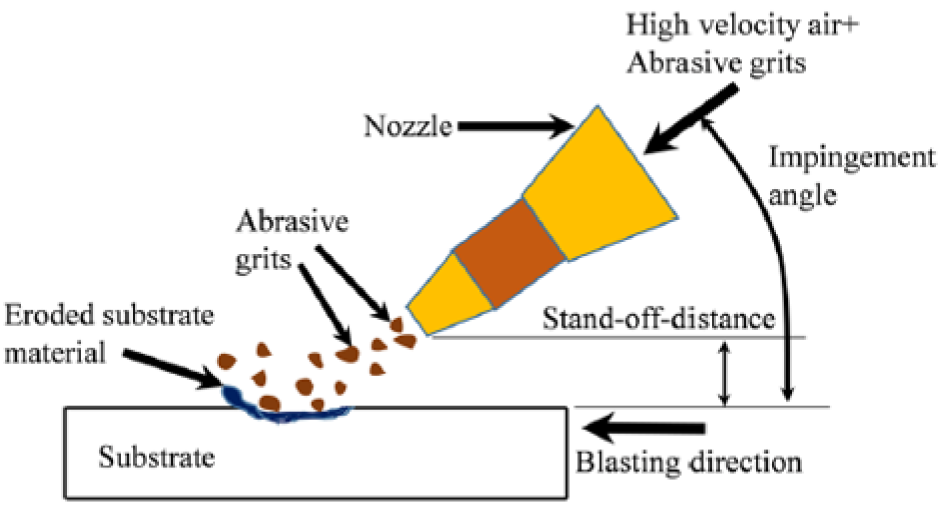

Figure 6: Schematic of grit blasting process (Ghara et al., 2021).

When grit blasting aluminium, special consideration needs to be given to the abrasive medium used. Common grit materials used with aluminium are alumina oxide, glass beads, or dry ice (Brewis *et al.*, 1999; Harris & Beevers, 1999; Possart *et al.*, 2002).

Testing has shown that grit blasting and cryoblasting, which uses dry ice as blasting medium, can reach single-lap shear strengths of 23.44 MPa and 22.10 MPa, respectively, but the strength decreases dramatically due to corrosion when aged (Brewis *et al.*, 1999; Harris & Beevers, 1999). This decrease in strength retention may be attributed to the rough surfaces created by grit blasting that allow for easier ingress of moisture to interact with the oxide layer, and this is supported by data that shows larger grit sizes create surfaces that have weaker bond durability (Critchlow & Brewis, 1995; Harris & Beevers, 1999).

2.2.4. Lasering

Lasering is an energetic physical pretreatment that uses a laser beam to clean and roughen a surface by partially melting it as can be seen in Figure 7 (Min *et al.*, 2020). The use of lasers in the surface modification of aluminium has become an effective replacement for wet pretreatments such as anodisation due to its comparable lap shear strength and excellent bond durability when aged (Broad *et al.*, 1999; Min *et al.*, 2020).

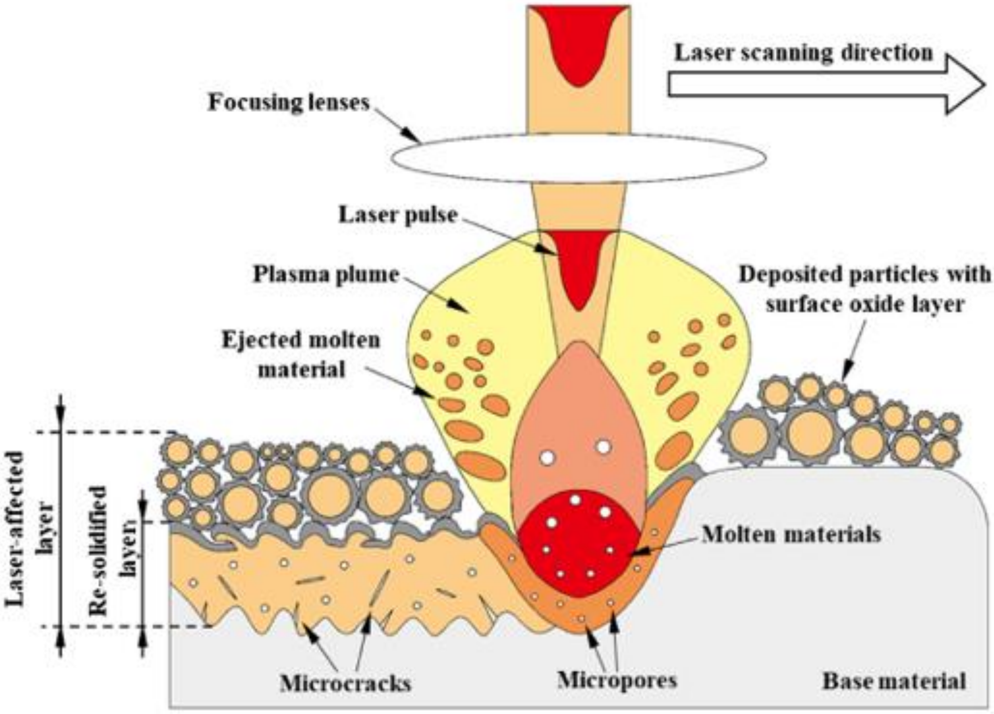

Figure 7: Schematic of lasering (Min et al., 2020).

As with anodisation, any changes to the input parameters such as pulse intensity and laser head speed, can lead to a difference in the microscopic surface structure from simply cleaning of contaminants to melting and transforming the surface morphology (Broad *et al.*, 1999; Rechner *et al.*, 2010; Reitz *et al.*, 2017). Unlike anodising, these variables are computer-controlled and highly repeatable, and using multiple axis CNC programming can accommodate various surface shapes and geometries (Orazi *et al.*, 2015). In addition, lasering is environmentally friendly and has a low maintenance cost (Broad *et al.*, 1999). Common bond strengths range from 17 MPa to 26 MPa, depending on laser input parameters (Min *et al.*, 2020; Rotella *et al.*, 2016). Lasering has also shown high resistance to ageing with bonds staying intact after more than 1400 days in a 100% humidity environment at 42-48 °C (Broad *et al.*, 1999).

2.2.5. Inorganic coatings

Solution gelation, also known as Sol-Gel, is a method used to create an interphase region between the epoxy and aluminium surface (da Silva *et al.*, 2018). This treatment combines an aqueous alkoxide solution with a silane coupling agent that forms strong covalent bonds with the appropriate primer or epoxy through the interphase region as seen in Figure 8 (da Silva *et al.*, 2018). This process can be combined with grit blasting to form bonds comparable to bonds formed on phosphoric acid anodised surfaces (da Silva *et al.*, 2018).

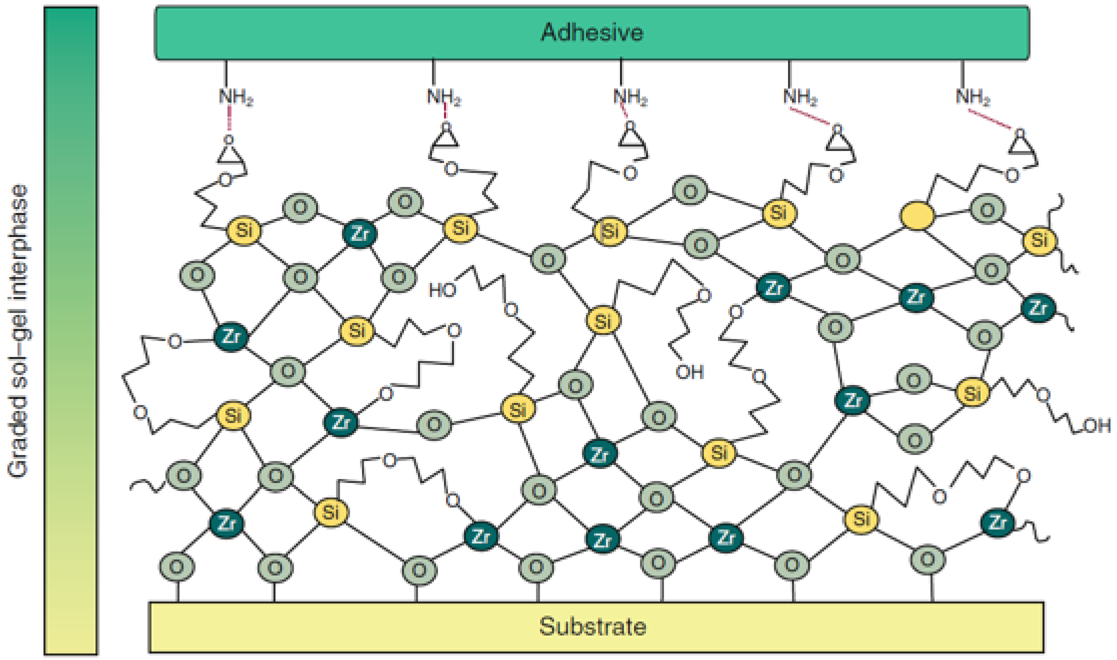

Figure 8: Schematic of interaction between adherend, adhesive and sol-gel interphase (da Silva et al., 2018).

2.3. Accelerated ageing

The accelerated ageing process artificially stresses joints over a comparatively short period in adverse conditions to simulate years of deterioration in a real-world scenario, even though there is no accurate correlation between hours aged and years of real-world usage (Cartwright, 2005; Council, 1996; Hutchinson, 1993). This ageing process is used to compare adherends that underwent differing surface pretreatments and is critical to fully characterising these treatments as some may initially show high shear strengths, but fare poorly when subjected to ageing (da Silva *et al.*, 2018). This bond stability is especially important in aircraft construction as they are expected to be in service for many years and thus bond durability is more important than actual adhesion strength (da Silva *et al.*, 2018:164). Hutchinson (1993:20) lists various ageing methods that include water, salt, and heat as variables. Some of these tests combine only heat and water and some only utilise a salt spray (Digby & Packham, 1995; Niknahad *et al.*, 2010). The most common method of accelerated ageing is to place samples in a chamber heated to 60 °C at a high relative humidity of up to 100% with some tests including the use of salt sprays or even complete immersion in water (Cartwright, 2005).

2.4. Standardised testing of adhesion strength

The effectiveness of surface pretreatments, choice of adhesive and adherends may be determined by established tests that are accurate and give reliable results. Regarding the testing of adhesion, it is vital to take note of the modes of failure namely adhesive or cohesive (Ebnesajjad & Landrock, 2015). The intermolecular forces and mechanical interlocking between different materials cause adhesion (da Silva *et al.*, 2018). Adhesive failure occurs when the adhesion forces between two materials are exceeded. In practice, adhesive failure occurs at the boundary between an adhesive and its adherend (da Silva *et al.*, 2018). Cohesion is caused by the intramolecular forces within each material and cohesive failure occurs when the cohesion forces within a single material are exceeded (da Silva *et al.*, 2018). In practice, this would be a failure within the adhesive or the adherend (da Silva *et al.*, 2018).

There are various methods by which adhesion can be tested, and each test serves a different purpose and has its unique challenges and advantages. Some of the most common tests are described in the following subsections.

2.4.1. Peel tests

Peel tests are conducted when it is necessary to determine the fracture energy of an adhesive bond between flexible adherends that may bend between 45° and 180° such as food packaging or electronic components (da Silva *et al.*, 2018). One of the most common peel tests is the T-peel test shown in Figure 9. This test is suitable for thin metallic adherends such as aluminium sheets (Broughton, 2000).

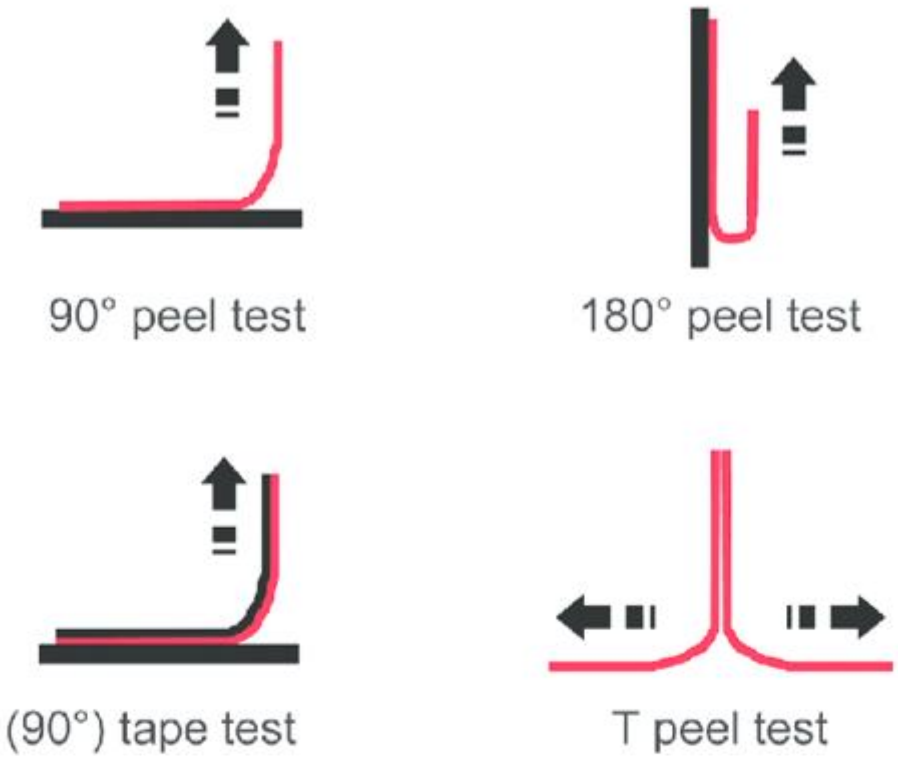

Figure 9: Schematics of various peel tests (Heinzmann et al., 2015).

2.4.2. Shear tests

One of the most common shear tests is the single-lap joint shear test, which consists of two rectangular tabs glued together with a certain overlap and bondline thickness (da Silva *et al.*, 2018). It is so widely adopted and accepted because it simulates adhesive joints in aerospace structures (da Silva *et al.*, 2018). These samples are then pulled apart with a tension and compression test instrument, and the strength required to break the adhesion is measured along with the strain endured by the sample (Xu *et al.*, 2016). This test is one of the most affordable and reproducible, but it does come with a caveat. When the adherends are pulled apart, a moment forms at the bond location due to the thicknesses of the coupons (da Silva *et al.*, 2018). The moment generated causes the joints to break in a mixed tensile and shear mode, thus not giving a pure shear result as shown in Figure 10.

A common standard for the lap shear joint test is ASTM D1002, and requires two coupons of metal with approximate dimensions of 100×25×1.6 mm that are adhered to each other with a 0.3 mm-thick layer of adhesive, with an overlap of between 12.5 and 25 mm (Cartwright, 2005; Duncan, 2010; Kuczmaszewski & Zawada-Michałowska, 2020; Udatha *et al.*, 2019). This single-lap joint is shown in Figure 11.

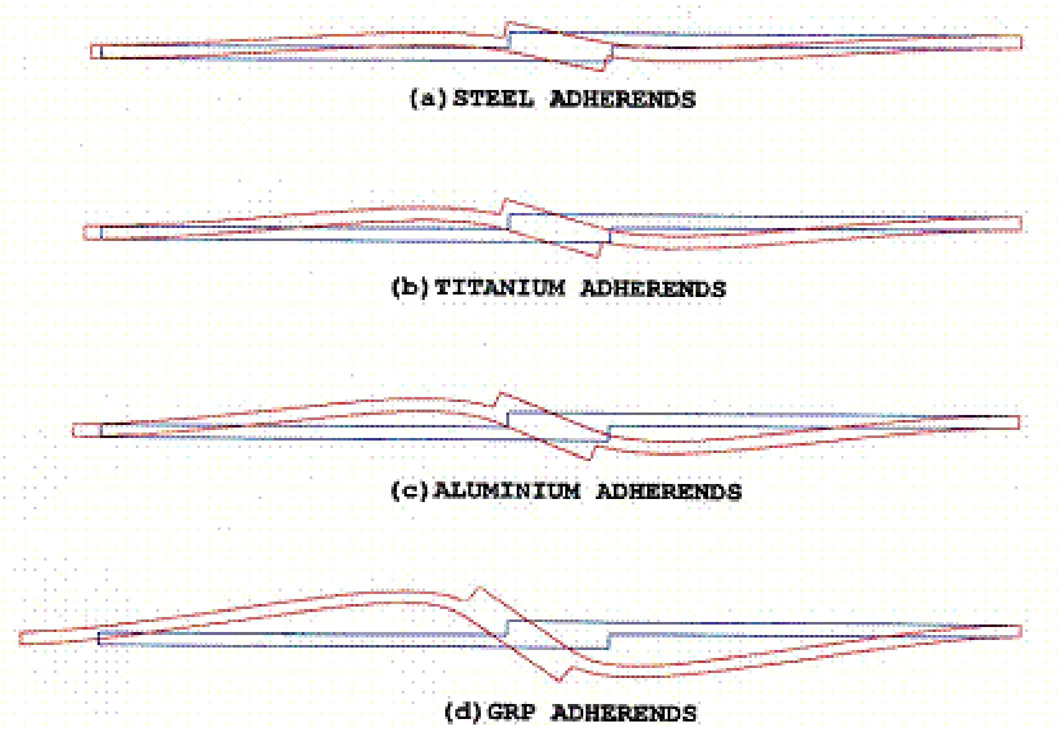

Figure 10: Single lap shear test moment (TWI, 2002).

Figure 11: Schematics single lap joint.

2.4.3. Tensile tests

A standard method of analysing the tensile strength of an adhesive is the butt joint test (da Silva *et al.*, 2018). This test has the adhesive in a thin layer between two substrates, as shown in Figure 12. The substrates are made of rigid materials such as steel where the thickness of the adhesive is controlled, and a mould is used to ensure that the adhesive is aligned correctly with the substrates. The drawback of this method is that if the adhesive and substrate are misaligned, then the axial load on the adhesive will cause bending, which would lead to incorrect measurements (da Silva *et al.*, 2018).

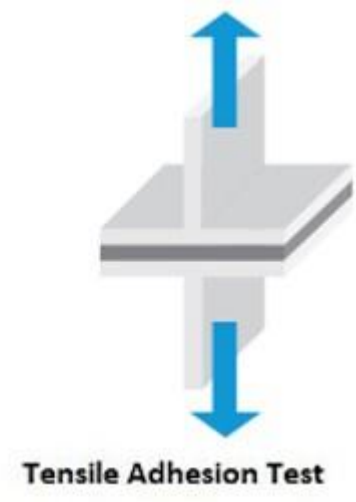

Figure 12: Schematic of tensile test (Saint-Gobain, 2020).

2.5. Conclusion

This literature review compared and described some of the most common theories, pretreatments, and testing methods used in adhesion. It has been shown that some pretreatments may provide similar results in one aspect but suffer in others. Anodising and grit blasting differ in cost, ease of use and repeatability and will be used to compare the strength and durability of aluminium bonded with epoxy. Accelerated ageing forms an integral part of any investigation on proper adhesion and thus will be included in this study. The single-lap shear test is one of the most common and widely reported methods of determining the bond strength of aluminium and epoxy and allows for many data points from which to draw meaningful conclusions.

3. Experimental method

In this section, the experimental method followed to test the bonding of aluminium and epoxy by anodising and grit blasting is discussed. The testing method is described, followed by the bond preparation steps and then the bonding process. Finally, the accelerated ageing process is explained.

3.1. Testing method

3.1.1. Lap shear testing

The lap shear test requires an increasing force to be applied to the bond sample until failure occurs. Servohydraulic test machines are typically used for this purpose. An MTS Landmark Servohydraulic Test System at the NWU Materials Laboratory was used in this study and is shown in Figure 13.

The deformation rate selected was 1.3 mm/minute, as it is in line with ASTM D1002. A sample size of 24, four batches of 6 samples, was selected for each PAA condition and 26, four batches of 7 samples, for each grit blasted condition. The chosen samples sizes exceeded typical sample sizes found for single lap joint testing in the literature where sample sizes are in the range of 3 to 6 for any given condition (Boutar *et al.*, 2016; Critchlow *et al.*, 2006; da Silva *et al.*, 2006; da Silva *et al.*, 2009). The difference in sample sizes chosen was because the anodising baths could only take 12 coupons at a time which equates to 6 samples whereas this restriction did not apply to the grit blasting. Furthermore, the adhesion jig could only take a maximum of 7 samples at a time for curing. This totalled 72 samples for all anodising conditions and 84 samples for all grit blasting conditions, where each batch of samples was created sequentially.

Figure 13: MTS Landmark Servohydraulic Testing System at NWU Materials Laboratory.

A custom alignment jig was developed to align the centre of the bond to the centre of MTS's claws, and minimise the moment caused in the joint, as shown in Figure 10 and explained in Section 2.4.2. The jig consisted of two machined carbon steel pieces inserted into the claws of the MTS machine. The samples were placed in the jig and fastened by a pressure plate using Allen head bolts. The jig mounted in the MTS system is shown in Figure 14. Complete drawings of the jig are given in Appendix A.

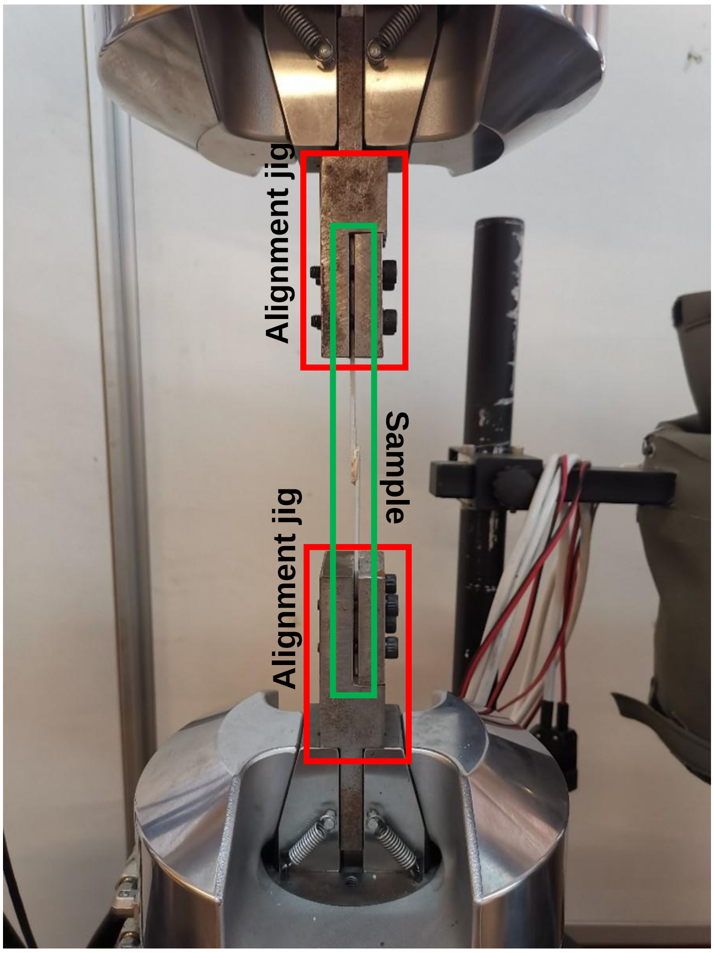

Figure 14: Alignment jig shown mounted in MTS system. The alignment jigs are in the red square and the sample is within the green square.

3.1.2. Visual analysis

Scanning Electron Microscopy, SEM, was chosen as a method of visual examination to show the microstructures on the surface of the aluminium and how well the adhesive adheres to these structures. An FEI Quanta 250 FEG SEM at the NWU Laboratory for Electron Microscope was used for this study. The working voltage and distance were set to 5-10 kV and 10 mm, respectively, after various imaging distances were examined. Visual analysis was also done using phone camera images to provide an understanding of the overall adhesion of the joint with regard to the adhesive and cohesive failure as explained in Section 2.4, as well as a degree of moisture ingress due to accelerated ageing as explained in Section 2.3. A Huawei Mate 20 smartphone was used to take images of the joints directly after failure of the joint on the MTS system.

3.2. Bond preparation

3.2.1. Anodising

The anodising process used was derived from a process by Digby and Packham (1995), but used acetone instead of 1,1,1 trichloroethane because the latter has been banned since 1996 due to its contribution to the depletion of the ozone layer (Information, 2023). Minco N24205 alkaline cleaner is not commercially available and was replaced with a sodium hydroxide etch. The post-anodising dip was removed because the available fume hood was not large enough to contain it, along with the anodising bath and heated etches. Digby & Packham (1995) showed that the post-anodising dip has a negligible effect on bond durability. An overview of the modified process is shown in Figure 15, the timings for each step are given in the procedure.

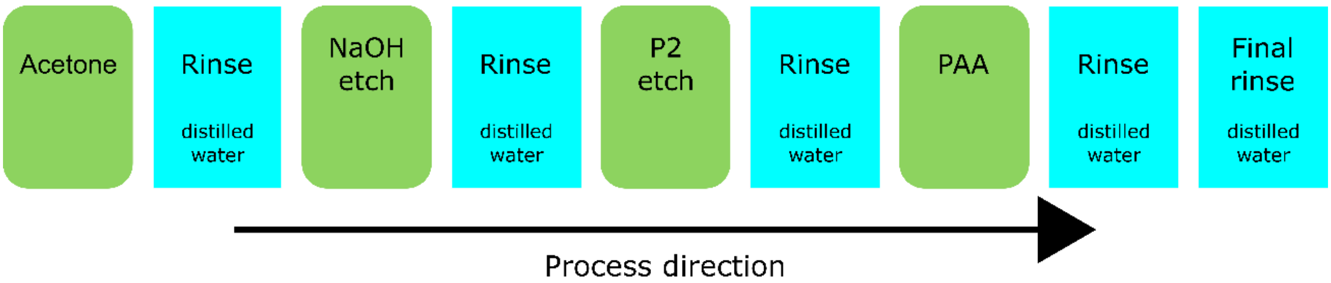

Figure 15: Anodising process line.

Acetone was used as a preliminary degreaser in container one along with distilled water in containers two, three, four and five. The etches fit between the rinses, with the NaOH etch being after the acetone step and the P2 etch after rinsing in container two as shown in Figure 15. The NaOH etch was a 3% solution of NaOH and the P2 etch was a 9 L solution of 3330 g of H_2SO_4 and 1350 g of ferric sulfate. These etches are shown in Figure 16. Both etches were heated to 60 °C and this, along with the corrosive nature of the etches, necessitated that they be placed in stainless steel containers. The reaction between NaOH and aluminium during etching releases hydrogen, and therefore the etching operations were all performed in a fume hood. The anodising step came after rinsing in container three and consisted of a 10% by-volume solution of phosphoric acid at room temperature with a constant voltage of 10 V on the power supply. The process ended with back-to-back rinses in containers four and five, followed by air drying.

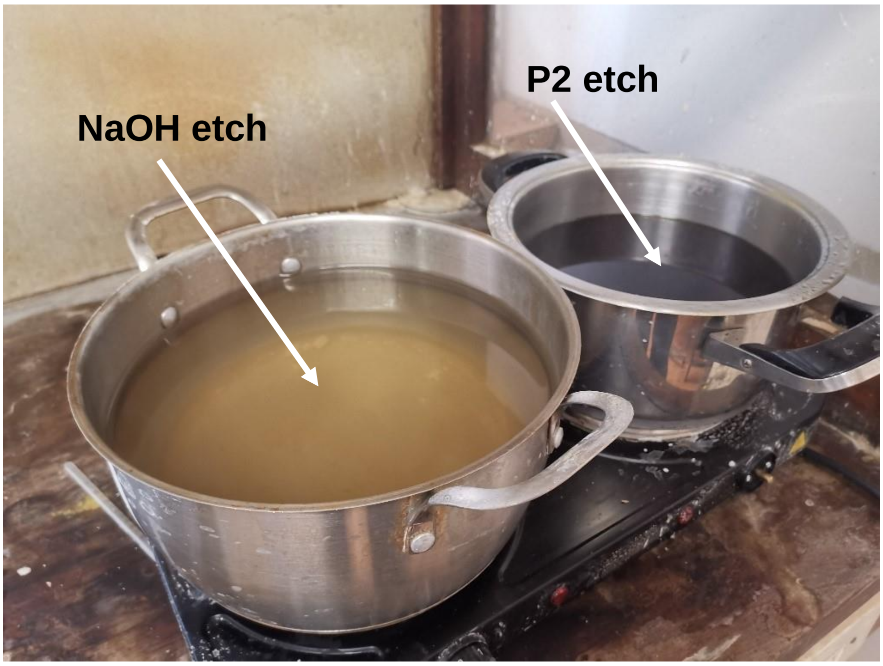

Figure 16: NaOH, left, and P2 etch, right

A schematic diagram of the anodising bath is shown in Figure 17. Two aluminium sheets were used as the cathode for the anodising bath because of their high corrosion resistance and high electrical conductivity. The bath was connected to a 12 V power supply by an insulated conductor rated to 3 A.

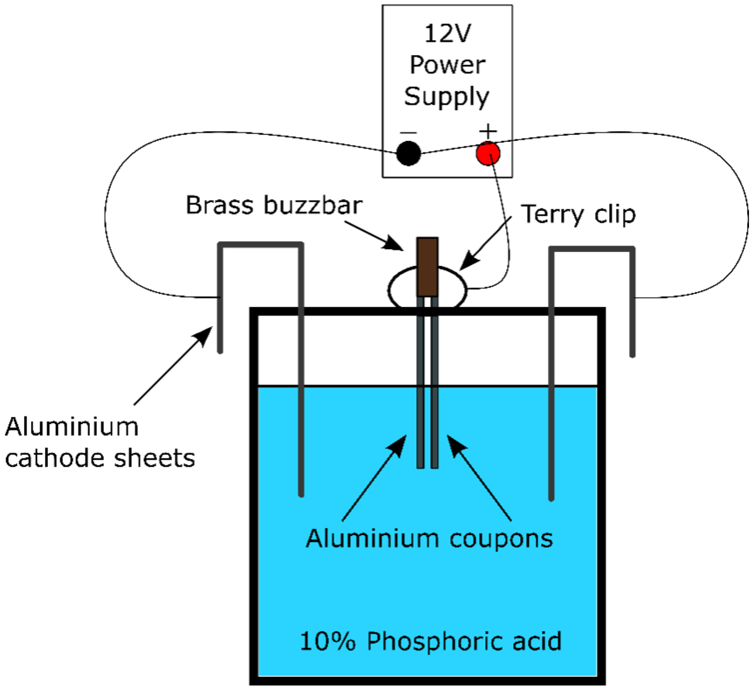

Figure 17: Schematic of anodising bath.

A brass busbar was used to attach the aluminium coupons during anodising. Brass was chosen for the busbar because of its high electrical conductivity and high corrosion resistance. Shallow slots were machined into the busbar at the same width as the coupons to hold them in place securely and prevent contact between the coupons. A CAD drawing of the busbar is shown in Figure 18, and complete drawings can be found in Appendix A.

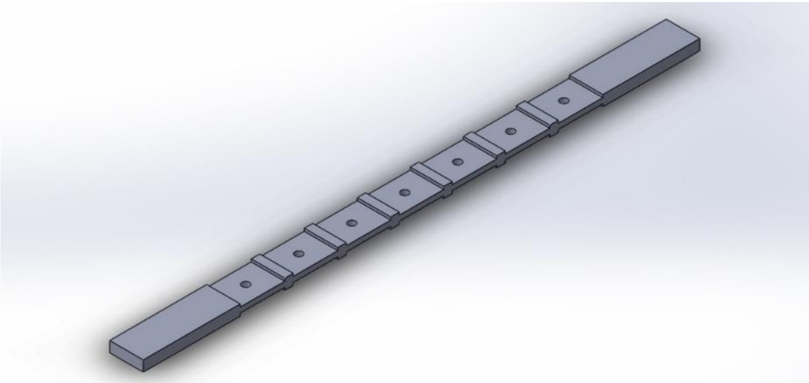

Figure 18: Brass busbar.

The busbar allowed easy manipulation of the coupons without touching them directly, which was especially important given that any contact with the treated surface of the aluminium could deposit oils and contaminants. Electrical contact with the busbar was made with terry clips, and these clips also held the busbar firmly in place. Figure 19 shows the anodising bath with a brass busbar and aluminium coupons fastened with brass nuts and bolts. The bath was tested, and bubbles formed on the surface of the aluminium coupons, confirming that anodising did take place.

Figure 19: Anodising bath.

3.2.2. Glass microsphere grit blasting

The grit blasting is as described in Section 2.2.3, with a stand-off distance of 10 cm, since this distance has previously been used as part of a grit blasting pretreatment (Arenas *et al.*, 2010; Possart *et al.*, 2002). The grit blasting was with a MAC AFRIC Bench Type Sand Blast Cabinet, as depicted in Figure 20, at Jonker Sailplanes in their prototyping hanger. The blasting was done by hand with an impingement angle of 90° and a dwell time of 30s. In addition, the 6 bar pressure of the blasting system and glass beads in the range of 150-250 µm was used by Possart (2002). The process ended with a rinse in acetone as a final degrease before air drying until all acetone had evaporated.

Figure 20: MAC AFRIC Bench Type Sand Blast Cabinet (Mart, 2023)

3.3. Sample bonding

The sample geometry was based upon the ASTM D1002 standard for testing metal-to-metal adhesion with epoxy. Changes were made to the joint overlap to compensate for the thickness of the material used. The standard requires samples that are approximately 101.6 mm long, 1.62 mm thick and 25.4 mm wide, but in this study, samples were 102 mm long, 2 mm thick, and 25 mm wide. The thickness of the bond was set to 0.3 mm, as it has been shown to yield the highest shear strength(Arenas *et al.*, 2010). Each joint sample tested was identified by its tag, BX, Y, where X is the batch number and Y is the sample number within the batch. For instance, B1,1 is batch 1, sample 1. Further explanation is given in Section 5.8 for these changes. A complete joint sample geometry is shown in Figure 21.

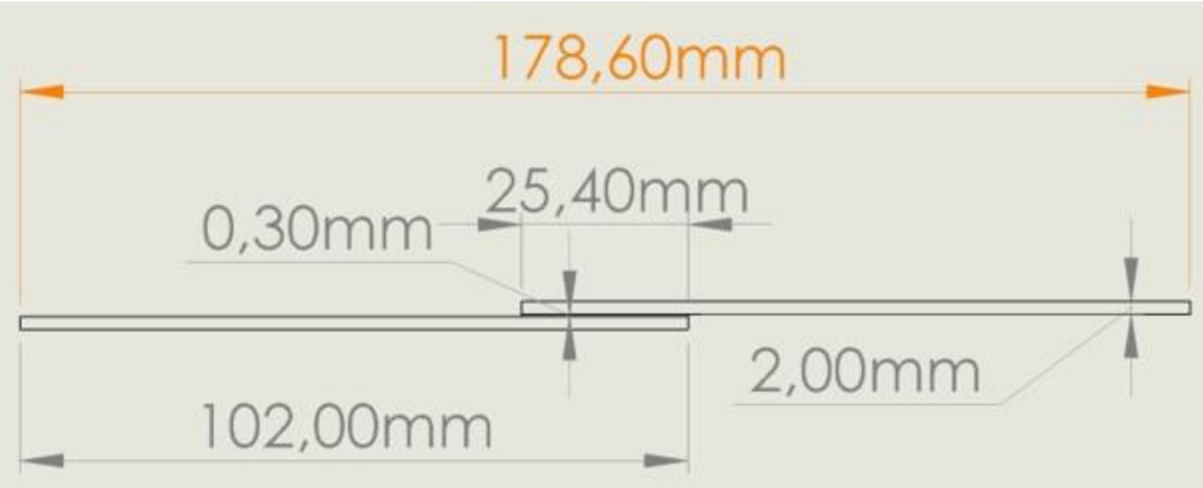

Figure 21: Joint sample geometry.

In this study a repeatable method for securing the specimens during bonding and curing was developed to ensure consistent results. A jig was designed based on some that are already used for such single-lap bonding(Technology, 2016). It was designed to keep the coupons straight and the adhesion area and bond line thickness constant. A visual representation of proper vs. improper alignment is given in Figure 22. The jig was made from plain carbon steel to provide a heavy, stable base that could be transported without disturbing the samples while curing. The alignment of the coupons and the constant adhesion area was achieved by holes drilled and tapped across the jig's surface and fastened with Allen head bolts, to act as stoppers. The bolts could be removed to safely demould the samples after curing.

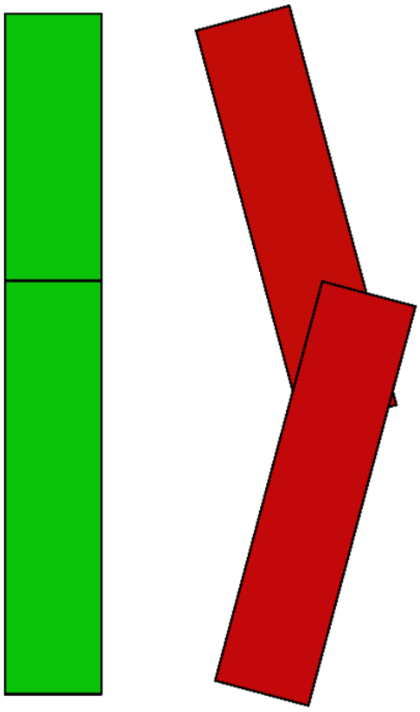

Figure 22: Proper vs. improper sample alignment.

A compression bar that spans the adhesion area to ensure consistent pressure was applied to each bond joint. As shown in light grey in Figure 23, the bar also had Allen head bolts that go through the holes drilled in it which fastened to the base, to locate the bar over the sample joint. The bar also had two grub screws in it that controlled the bond line thickness, because the bar could only be tightened until the grub screws contacted the jig base.

The thickness was set with two aluminium coupons and a 0.3 mm feeler gauge. The coupons were stacked on top of each other under the bar on the lower step of the base, and the feeler gauge was inserted between the top coupon and the bar. The grub screws were adjusted until the feeler gauge contacted the bar. Thread locker was added to the grub screws to prevent them from moving. The CAD design for this jig is shown in Figure 23. Detailed drawings of the jig can be found in Appendix A.

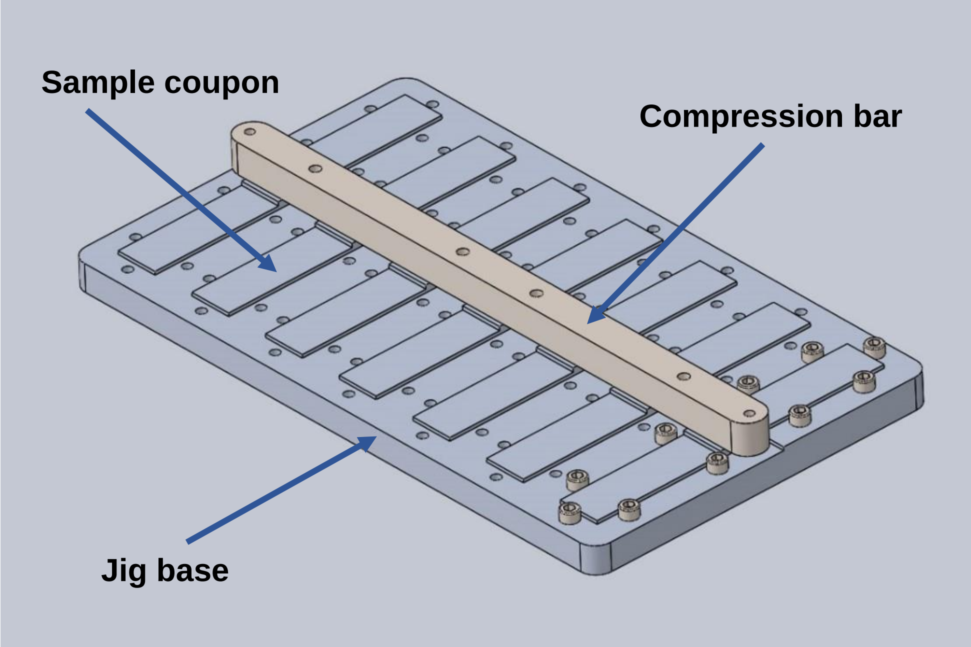

Figure 23: Adhesion alignment jig CAD model with coupons

The area on the jig base where the overlap occurred was polished to a mirror surface to ease the demoulding process. A layer of grease spray was also applied to the surface of the jig to further ease demoulding. This was necessary because in the adhesion process, some of the epoxy spilled out of the sides of the bond, which ensured that the entire intended adhesion surface area was covered with adhesive. Figure 24 shows the completed jig without coupons.

Figure 24: Adhesion alignment jig without any coupons

3.4. Accelerated ageing

Accelerated ageing was done as discussed in Section 2.3. A polypropylene container was used for the ageing, as it could handle the 60 °C temperature and would not corrode in the salt solution. The container was filled with 75 L of plain tap water and 2.25 kg of sodium chloride to create a 3% salt water solution to be heated to 60 °C, as done by Del Real (2006). The solution was heated with a stainless-steel heating element equipped with a stirrer and a thermostat. The ageing bath with immersed samples can be seen in Figure 25.

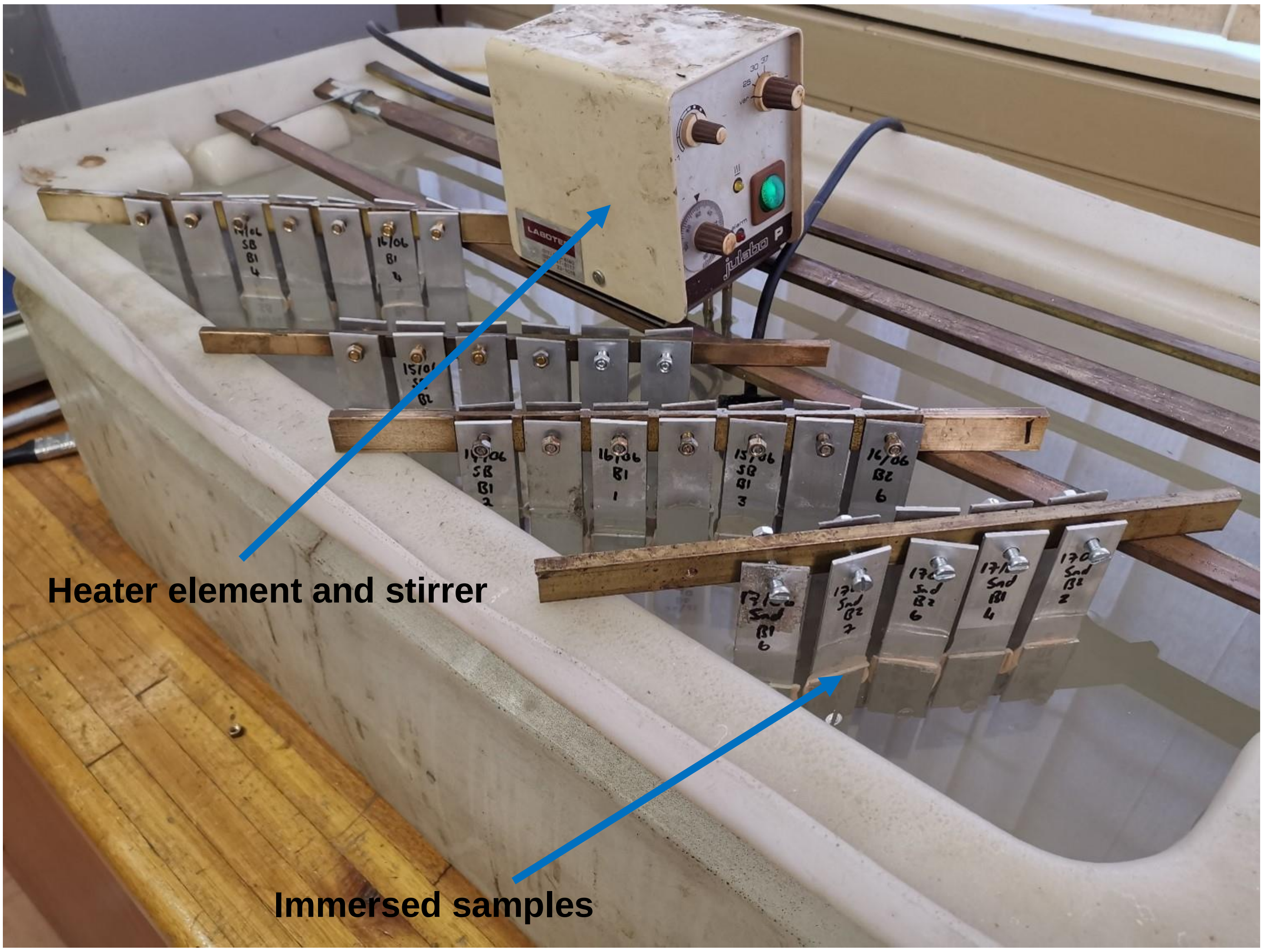

Figure 25: Accelerated ageing bath with joint samples.

4. Experimental procedure and testing

4.1. Anodising

The following procedure was followed to anodise aluminium coupons in preparation for bonding. All electrical contact points on the busbar were cleaned using steel wool before every session of anodising to ensure a proper electrical connection.

1. Untreated aluminium coupons were immersed and agitated in pure acetone to remove surface oils.
2. The coupons were submerged in the NaOH etch for 10 minutes, after which they were rinsed in distilled water.
3. The coupons were then placed in the P2 acid etch for 10 minutes and subsequently rinsed with distilled water.
4. The coupons were then placed in the anodising bath for 20 minutes.
5. The specimens were then rinsed in two separate distilled water baths to remove all chemicals and residue.
6. Specimens were then air-dried in preparation for adhesion.

4.2. Grit blasting

The following procedure was followed to grit blast the aluminium coupons.

1. Grit blasting was done on identical specimens as used for the anodising.
2. Glass microspheres with a size range of 150-250 microns were used to clean the aluminium specimens' surfaces of any possible contaminants.
3. Attention was given to ensure a consistent dwell time over and distance from the aluminium coupons during blasting.
4. The coupons were subsequently rinsed in pure acetone to remove any leftover glass microspheres and oils on the surface.
5. The acetone was allowed to evaporate in preparation for adhesion.

4.3. Bonding

Single-lap joints were bonded in the alignment jigs using SpaBond 345 (Gurit) resin (yellow), with the appropriate slow hardener (red), at a 100:40 ratio by weight, as recommended by the manufacturer. The joint samples were cured in the adhesion alignment jig for 24 hours at 25 °C before being demoulded and subsequently heat-treated at 70 °C for 5 hours, per the manufacturer's specifications, to obtain maximum bond strength and durability.

4.4. Ageing

The samples were fastened to the brass busbars and suspended in the solution on longer brass bars that spanned the length of the container, as shown in Figure 25. Anodised and grit-blasted joint specimens were submerged for 300 and 600 hours, respectively. These times were chosen because they fall within the typical amount of time usually taken to age aluminium-epoxy bonds (Niknahad *et al.*, 2010; Xu *et al.*, 2016). This setup was covered with cellophane wrap to reduce moisture loss during the ageing time. The bath was topped up with water as necessary. After the allotted time passed, the specimens were rinsed with clean water and air-dried in preparation for testing.

5. Results and discussion

5.1. Introduction

The results of this study were categorised into two main parts: quantitative and qualitative. The quantitative data included the comparison of lap shear strengths for anodised and grit blasted joints, both unaged and after ageing for 300 and 600 hours, along with a statistical analysis of the lap shear strengths and the influence of the associated confidence levels. The qualitative data consisted of optical and SEM analysis of the prepared surfaces and the fractured surfaces, both unaged and aged. Lastly, verification and validation were discussed.

A summary of the results was given in the form of a box-and-whisker plot in Figure 26. For context, shear strength values were calculated by taking the load applied in Newtons and dividing it by the surface area of the bond in mm^2. The formula is given below:

$$\sigma = \frac{F}{A} = \frac{N}{mm^2} = MPa$$

This plot showed the outliers associated with both PAA and grit blasting as well as the mean, Q1, Q3, minimum and maximum values of lap shear strength. The 0 hours aged PAA results had one outlier on the upper end of the plot. The 300 hours aged PAA results had one outlier on the upper end of the plot and one outlier at the lower end of the plot. There was one outlier on the lower end of the plot for 300 hours aged grit blasting and one outlier on the lower end of the plot for 600 hours aged grit blasting. The outliers for grit blasting are associated with complete failure of the adhesive bond due to ageing and was further discussed in the qualitative analysis of the results.

These outliers were removed to ensure that the data may be fairly interpreted, but the grit blasting outliers were considered significant because such outliers were not encountered with PAA. This observation formed an important part of the of the comparison of the two pretreatment methods.

The presence of outliers skewed the data and thus nullified any basic statistical analysis on the data to determine true differences in means (McDonald, 2009). For this reason, the outliers for both PAA and grit blasting identified in the box-and-whisker plot were removed. To further support this decision the Jarque-Bera test was used to determine normality of the result distributions.

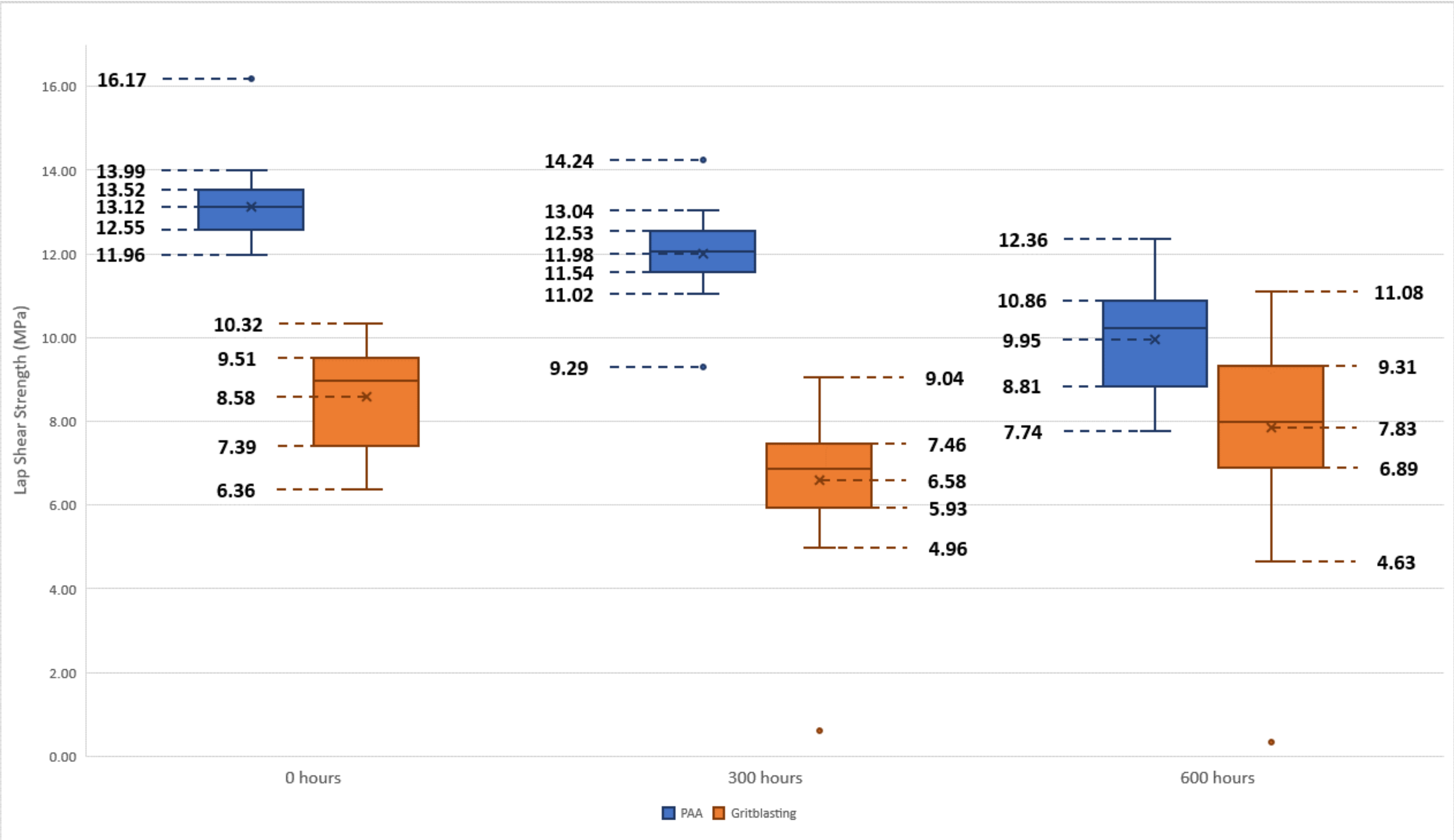

Figure 26: Summary of lap shear strengths with box and whisker plots

The Jarque-Bera test was used for testing normality and these results are presented in Table 1 before and after outliers were removed. The Jarque-Bera test uses the number of samples as well as the kurtosis and skewness of the results to conclude on distribution normality (Jarque & Bera, 1987). The test's null hypothesis is that the distribution is normal. Thus, if the *p*-value from the test is higher than the significance level, which in this case is 0.05, then the null hypothesis cannot be rejected, and it can be assumed that the distributions are sufficiently normal (Jarque & Bera, 1987). It is thus clear from Table 1 that after outliers have been removed all distributions are assumed to be normal and tests may be performed on the results. The removal of the outliers did reduce the number of samples available for each testing condition, but all the statistical tests applied account for differences in sample size.

Table 1: Jarque-Bera test results with and without outliers

	***p*-value w/ outliers**	***p*-value w/o outliers**
PAA 0 hours	1.54E-10	0.59
Gritblasting 0 hours	0.33	N/A
PAA 300 hours	8.24E-04	0.73
Gritblasting 300 hours	1.16E-16	0.83
PAA 600 hours	0.63	N/A
Gritblasting 600 hours	1.17E-08	0.86

With the outliers removed and the distributions assumed to be normal further analysis was conducted for each of the surface pretreatments. Welch's *t*-test was chosen in place of the typical Student's *t*-test to test for a significant difference between means because it is more resistant to changes in sample variance and sample size (Delacre *et al.*, 2017). Given that there were differences in both sample variance and size of this study's results, Welch's *t*-test provided better insight into the significance of each pretreatment's mean lap shear strengths. Welch's t-test was used to compare each aged condition within each pretreatment to determine whether ageing caused a significant change in the mean lap shear strengths. Furthermore, each aged condition for PAA was compared to the corresponding grit blasting aged condition to determine whether the differences in mean lap shear strengths between pretreatments were significant. For comparison, one set of results was used to show the differences in these two *t*-tests.

5.2. Phosphoric acid anodising

Table 2 reported various statistical parameters applicable to PAA results. Conditional formatting was applied to easily rank results according to their criterion. For example, a high mean was desirable and thus was identified with green, whilst a high variance was undesirable and was indicated with red. The 0 hours aged samples were strongest with a mean of 12.982 MPa and 600 hours aged samples were weakest with a mean of 9.949 MPa. The standard error for the 600 hours aged samples was 2.185 and 2.316 times greater than that of the 0 hours and 300 hours aged samples respectively. Welch's test was applied to these three sets of data to determine whether the difference in means was indeed significant.

Table 2: Summary of statistical parameters for anodised samples

	PAA 0hrs	***PAA 300hrs***	***PAA 600hrs***
Mean	12,982	11,996	9,949
Standard Error	0,124	0,117	0,271
Median	13,093	12,049	10,208
Standard Deviation	0,593	0,547	1,327
Sample Variance	0,351	0,299	1,762
Range	2,029	2,016	4,614
Minimum	11,957	11,019	7,741
Maximum	13,986	13,035	12,355
Count	23,000	22,000	24,000
Confidence Level (95.0%)	0,256	0,242	0,560
Confidence Level (99.0%)	0,348	0,330	0,761

Welch's test was applied three ways between any two anodised conditions as shown in Table 3. The significance level, or alpha value, was chosen as 0.05 and a difference in means is significant when the *p*-value is lower than this alpha value. Table 3 shows that there is a significant difference between any three anodised conditions.

Table 3 Welch's test results for anodised samples

PAA			
	0hrs vs 300hrs	**300hrs vs 600hrs**	**0hrs vs. 600hrs**
Alpha	0,05	0,05	0,05
F-stat	33,71	48,18	103,79
df1	1	1	1
df2	42,95	31,14	32,11
p-value	7,03E-07	8,51E-08	1,38E-11
Significant	yes	yes	yes

To further show the behaviour of the samples under testing conditions stress vs. strain graphs were drawn and shown below for each ageing condition. Unfortunately, all raw data for the unaged samples became corrupted and unrecoverable. Figure 27 shows stress vs. strain for 300 hours aged anodised samples and each samples underwent a slight yield as indicated by the change in slope of the line. Run 1 and 6 did not reach 0 MPa because the testing machine stopped after detecting a break and the coupons were still attached to each other by a sliver of epoxy, so the runs were still counted as valid.

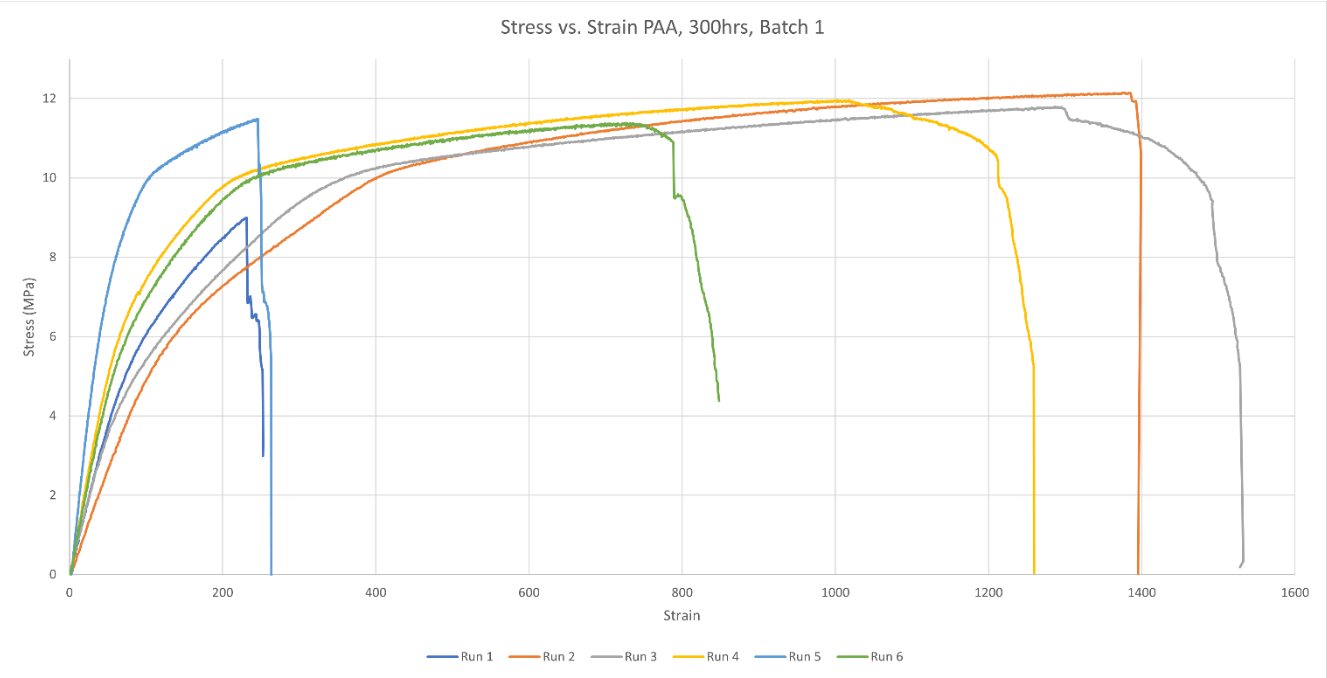

Figure 27 Stress vs. Strain for PAA samples aged 300 hours

Figure 28 shows that at 600 hours the samples had more pronounced yield points with shorter elongations on average compared to the 300 hours aged samples.

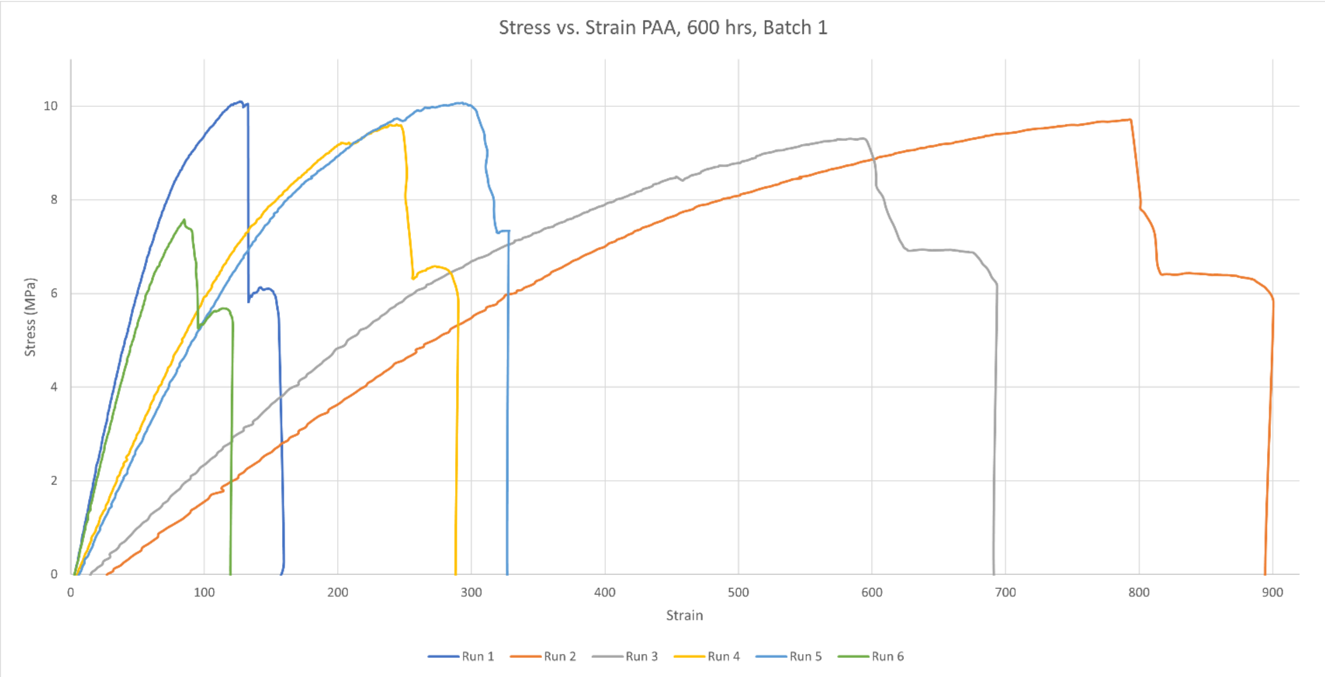

Figure 28 Stress vs. strain for PAA samples aged 600 hours

Given that there were 4 batches for each pretreatment and ageing condition it was important to consider potential differences. To do this Welch's test was once again applied and showed that for unaged samples there were no significant differences in mean values as seen in Table 4. The same was true for the 300 hours aged samples, but there was a difference within batches for the 600 hours aged samples.

Table 4 Interbatch Welch's test for PAA

PAA interbatch			
	0hrs	**300hrs**	**600hrs**
Alpha	0,05	0,05	0,05
F-stat	2,97	1,77	8,73
df1	3	3	3
df2	9,12	9,69	10,65
p-value	8,86E-02	2,18E-01	3,27E-03
sig	no	no	yes

5.3. Grit blasting

In Table 5 the summary of statistical parameters for grit blasting was given. As in Table 2 conditional formatting was applied to emphasize results. The 0 hours aged samples were the strongest with a mean of 8.575 MPa and the 300 hours aged samples the weakest with a mean of 6.899 MPa. The mean strength increased from 300 to 600 hours by 1.25 MPa which is contradictory to the results from the PAA samples, but this phenomenon was also reported by Harris & Beevers (1999). The standard error of the 600 hours aged samples was 1.309 and 1.451 times greater than the 0 hours and 300 hours aged samples respectively. Welch's test was applied to these three sets of data to determine whether the difference in means was indeed significant.

Table 5: Summary of statistical parameters for grit blasted samples

	GB 0hrs	GB 300hrs	GB 600hrs
Mean	8,575	6,800	8,107
Standard Error	0,233	0,206	0,305
Median	8,942	6,882	8,150
Standard Deviation	1,234	1,072	1,585
Sample Variance	1,524	1,148	2,512
Range	3,960	4,090	6,451
Maximum	10,318	9,045	11,078
Minimum	6,358	4,955	4,627
Count	28,000	27,000	27,000
Confidence Level (95.0%)	0,479	0,424	0,627
Confidence Level (99.0%)	0,646	0,573	0,848

Welch's test was applied three ways between any two grit blasted conditions as shown in Table 6. The significance level, or alpha value, was chosen as 0.05 and a difference in means is significant when the *p*-value is lower than this alpha value. Table 6 shows that there is a significant difference between the 0 hrs and 300 hrs and 300 hrs and 600 hrs aged samples, but not as significant between 0 hrs and 600 hrs aged samples.

To further show the behaviour of the samples under testing conditions stress vs. strain graphs were drawn and shown below for each ageing condition. The graphs are shown in Figure 29 to Figure 31. On average they show lower strain values than the anodised joints. The maximum strain values also followed the trend of the stress values where the strain was highest for unaged joints, lowest for 300 hours aged joints and in between for 600 hours aged joints.

Table 6 Welch's test results for grit blasted samples

Grit Blasting			
	0hrs vs. 300hrs	300hrs vs. 600hrs	0hrs vs. 600hrs
Alpha	0,05	0,05	0,05
F-stat	32,50	12,60	1,49
df1	1	1	1
df2	52,44	45,66	49,12
p-value	5,55E-07	9,08E-04	2,29E-01
sig	yes	yes	no

Welch's test was also applied to the different grit blasted batches and the results are given below in Table 7. There are significant differences in the interbatch mean values for all the ageing conditions. This could be attributed to the variance in grit blasting results that have already been presented.

Table 7 Interbatch Welch's test for grit blasting

Grit Blasting interbatch			
	0hrs	300hrs	600hrs
Alpha	0,05	0,05	0,05
F-stat	28,58	13,78	20,53
df1	3	3	3
df2	13,04	12,00	11,46
p-value	5,29E-06	3,41E-04	6,56E-05
sig	yes	yes	yes

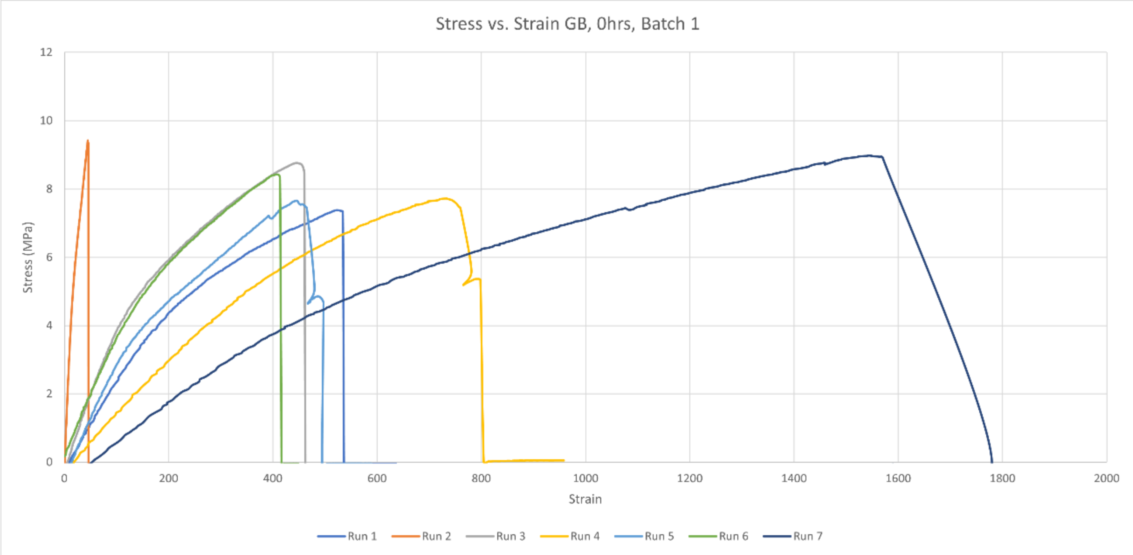

Figure 29 Stress vs. strain for grit blasted samples aged 0 hours

Figure 30 Stress vs. strain for PAA samples aged 300 hours

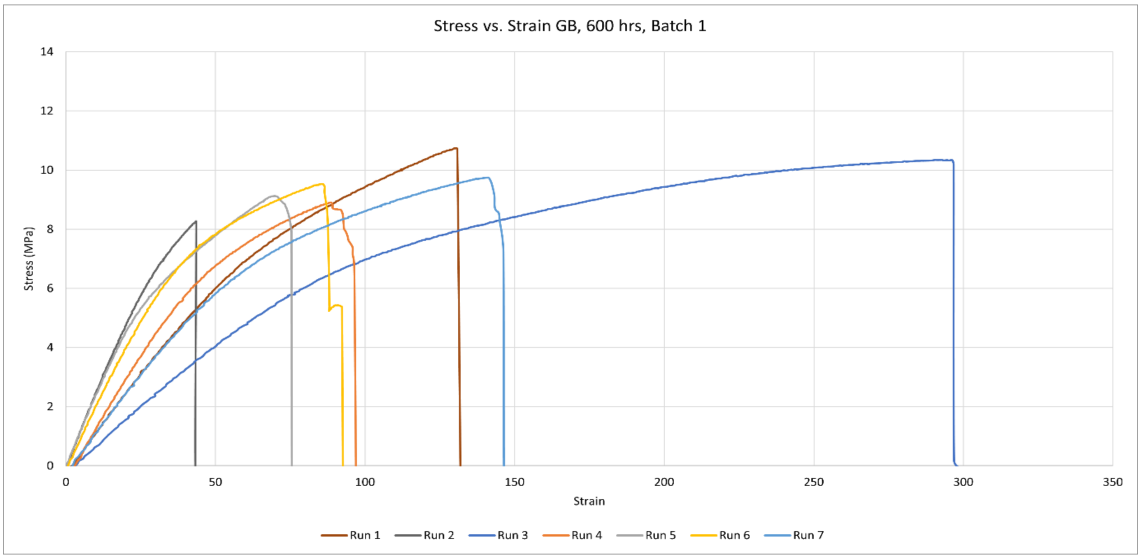

Figure 31 Stress vs. strain for grit blasted, 600 hours aged joints

5.4. Phosphoric acid anodising compared to grit blasting

When PAA was compared to grit blasting in Table 8, it was observed that overall PAA samples performed better under each condition than the grit blasted samples. Some notable differences between the two pretreatments included the sample variance at 0hrs and 300hrs aged as well as the mean values for all ageing conditions.

Table 8 Summary of statistical parameters between PAA and grit blasting

	PAA 0hrs	PAA 300hrs	PAA 600hrs	GB 0hrs	GB 300hrs	GB 600hrs
Mean	12,982	11,996	9,949	8,575	6,800	8,107
Standard Error	0,124	0,117	0,271	0,233	0,206	0,305
Median	13,093	12,049	10,208	8,942	6,882	8,150
Standard Deviation	0,593	0,547	1,327	1,234	1,072	1,585
Sample Variance	0,351	0,299	1,762	1,524	1,148	2,512
Range	2,029	2,016	4,614	3,960	4,090	6,451
Minimum	11,957	11,019	7,741	6,358	4,955	4,627
Maximum	13,986	13,035	12,355	10,318	9,045	11,078
Count	23,000	22,000	24,000	28,000	27,000	27,000
Confidence Level (95.0%)	0,256	0,242	0,560	0,479	0,424	0,627
Confidence Level (99.0%)	0,348	0,330	0,761	0,646	0,573	0,848

Furthermore, Welch's test was applied to compare the two pretreatments at each ageing conditions and the results were given in Table 9 below. This shows that for each ageing condition there is a significant difference in the mean values of PAA compared to grit blasting.

Table 9 Welch's test results where PAA was compared to grit blasting

PAA vs. Grit Blasting			
	0hrs vs. 0hrs	300hrs vs. 300hrs	600hrs vs. 600hrs
Alpha	0,05	0,05	0,05
F-stat	278,74	481,04	20,38
df1	1	1	1
df2	40,38	40,19	48,84
p-value	0,00E+00	0,00E+00	4,02E-05
sig	yes	yes	yes

5.5. Optical analysis of fractured surfaces

Visual analysis of the unaged fracture surfaces gave a qualitative complement to the quantitative data shown in Sections 5.2 to 5.4. The grit-blasted surface on the left of Figure 32 showed a clean fracture within the epoxy and the surface of the aluminium for both surface pretreatments. This was adhesive failure between the aluminium and epoxy, but also a cohesive failure within the epoxy and was thus considered a mixed failure mode. Further cohesive failure was circled within Figure 32 in the anodised joint, and this showed that the bond between the anodised surface and the epoxy was stronger than the internal bonds of the epoxy to itself (da Silva *et al.*, 2009:164). This kind of failure was very desirable and was indicative of a very strong adherend-to-adhesive bond. Such cohesive failures, as circled in red in Figure 32, were not noted in any of the unaged grit-blasted joints.

Figure 32: Fractured surfaces of unaged joints grit blasted and anodised

Figure 33 shows the fractured surfaces of a grit-blasted and anodised joint, left and right respectively, after 300 hours of ageing. The aged, anodised joint was like the unaged joint, and there was no apparent difference between the 0 hours and 300 hours aged joints. In contrast, it was evident that there was some interaction between the salt water and grit blasted samples as indicated by the red circle where a white discolouration could be seen on the surface of the aluminium. This could have been moisture infiltration along with precipitation, but this was inconclusive without compositional analysis. However, the discolouration was useful as a metric to compare anodising to grit blasting as no 300 hours aged anodised samples showed this discolouration.

Figure 33: Fractured surfaces of 300 hours-aged joints.

It was apparent that 600 hours of exposure to heated salt water had detrimental effects on both the anodised and grit-blasted joints, as seen in Figure 34. There was an evident change in the 600 hours aged fracture surface of this grit blasted joint compared to an unaged grit blasted joint. White discolouration on the surface could have been attributed to a change in morphology and composition. This discolouration could have been attributed to ingress of moisture and salt into the bond, which led to its ultimate failure. The anodised joint experienced similar discolouration of its surface that was different when compared to either the 0 hours or 300 hours aged samples. This was an excellent example of the durability of anodised joints because none of them showed the same discolouration and change to the surface as the grit blasted joints showed. The shear strengths for the joints shown in Figure 34 were the lowest recorded after 600 hours of ageing at 0.32 MPa and 5.50 MPa for the grit-blasted and anodised joints, respectively.

Figure 34: Fractured surfaces of 600 hours-aged joints.

Figure 35 shows two fracture surfaces that show no apparent signs of discolouration or changes to the fractured joint surface after 600 hours of ageing. The anodised joint on the right in Figure 35 shows a typical example of cohesive failure, circled in red, with epoxy visible on corresponding sides of the joint. The grit blasted joint also showed a combination of adhesive and cohesive failure and indicated that it could provide resistance to ageing, albeit to a lesser extent than anodising.

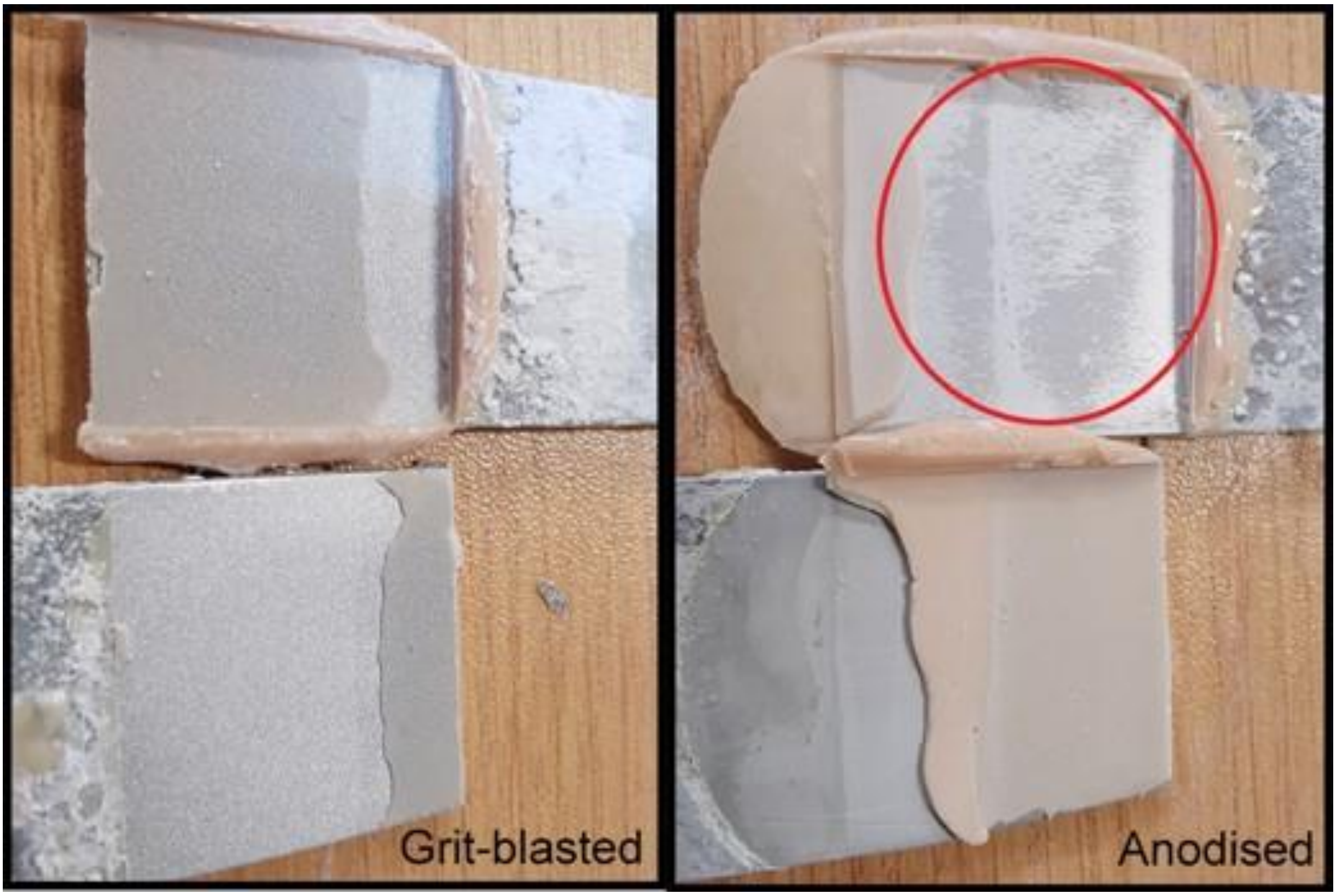

Figure 35: Fractured surfaces of 600 hours-aged joints with no apparent moisture ingress.

Optical analysis showed that the anodised joints were better at adhering to the epoxy as indicated by the cohesive failure areas where epoxy could be seen on corresponding sides of the fractured joint, while this type of failure was not seen on any of the grit-blasted joints. The anodised joints were also more resistant to ageing because the worst aged, anodised joint showed less apparent moisture ingress and damage than the worst aged grit-blasted joint.

Finally, a phenomenon known as stress whitening was seen on the anodised samples The type of joint failure; be it adhesive failure (AF), cohesive failure (CF) or a combination of the two (AF + CF), along with the corresponding frequencies are given in Table 10. The anodised samples at 300 and 600 hours aged conditions remained consistent in the type of failure whilst grit blasted joints declined in mixed failure to adhesive failure from 0 hours aged to 600 hours aged. As previously discussed, this is due to a weaker bond between the grit blasted surface and the epoxy than the bond within the epoxy.

Table 10 Joint failure type and frequency

	PAA			Grit Blasting		
	AF	AF + CF	CF	AF	AF + CF	CF
0hrs	0%	54%	46%	21%	79%	0%
300hrs	17%	83%	0%	39%	61%	0%
600hrs	13%	88%	0%	54%	46%	0%

5.6. Analysis of treated surfaces by SEM

SEM analysis was done for a selection of unaged, 300 hours-aged and 600 hours-aged joints that were grit-blasted and anodised. Only two of each ageing condition for each pretreatment were analysed by SEM, but the locations for imaging were based on how they represented different characteristics such as surface structure, moisture ingress and whether adhesive was still on the surface or not.

SEM analysis showed a difference in surface morphology of grit-blasted and anodised aluminium that was not apparent through optical analysis. Figure 36, at 250× magnification, shows that the grit-blasted surface was relatively smooth with some random slivers of aluminium sticking out from the surface, whilst the anodised surface had a pitted and rougher surface. The anodised pattern consisted of smaller pores and deeper crevasses all over the surface along the grain boundaries. The very fine patterns of the anodised surface explain why it was dull to the naked eye, as light was not fully reflected but rather refracts in between the pores.

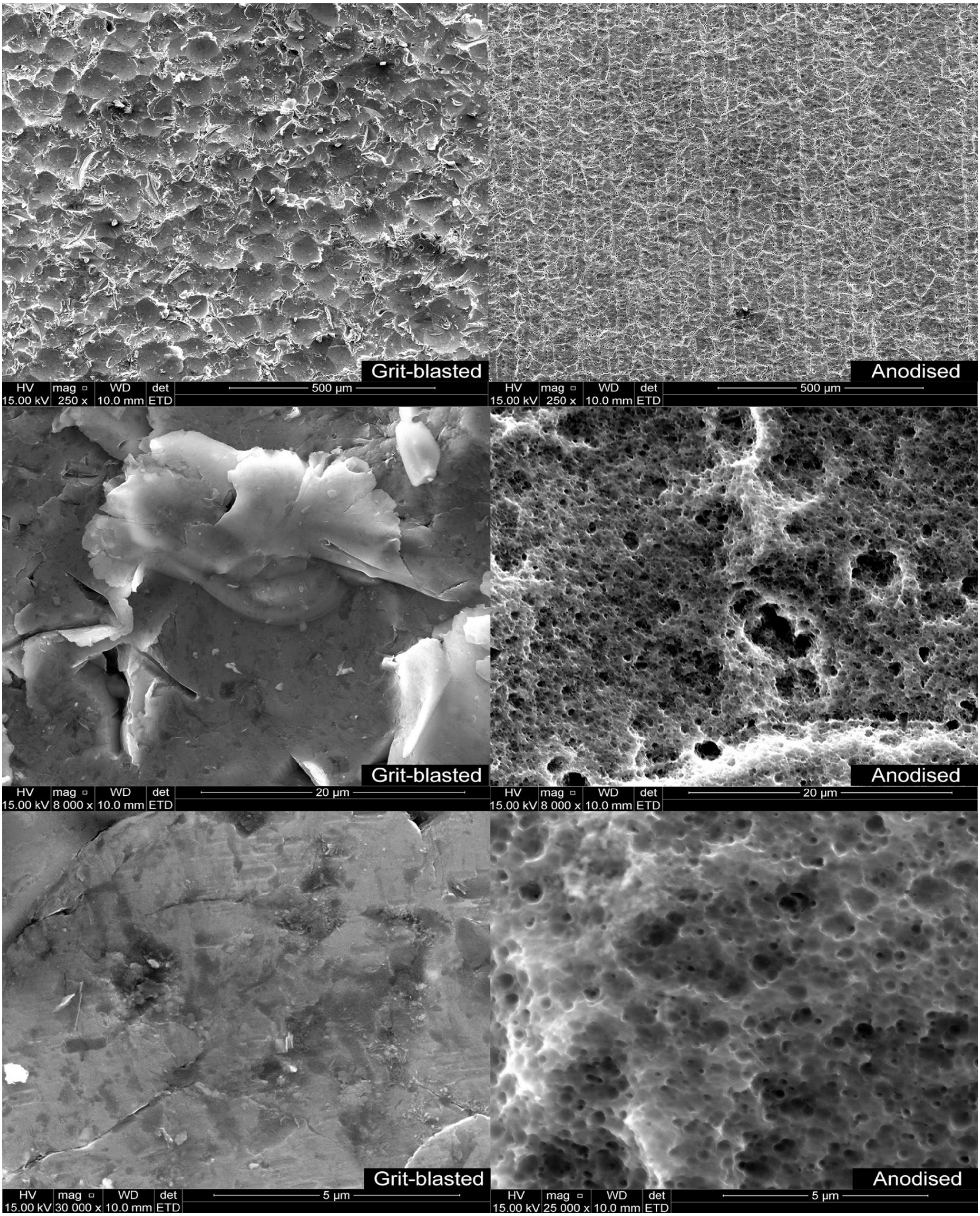

Figure 36: Treated aluminium surfaces under various levels of magnification

Magnification at 8000× in Figure 36 showed micron-sized holes in the anodised surface into which epoxy could flow to seal the surface from moisture ingress and interlock with the aluminium, which lead to greater adhesion strength. As previously noted, the grit-blasted surface was comparatively smoother than the anodised surface, with slivers sticking up from the surface. The aluminium slivers would have provided some mechanical interlocking with the epoxy, but the rest of the surface was too smooth to provide the same adhesion as seen with the anodised surface.

At 30,000× magnification in Figure 36, the pores produced by the anodising could be seen and even measured. The pores ranged in size from 150 nm to 420 nm, consistent with what was found in previous studies (Cartwright, 2005; Goushegir *et al.*, 2020; Li *et al.*, 2019; Xu *et al.*, 2016). Sharp edges on the borders of the pores could also be seen, which would further improve interlocking with the epoxy.

5.7. Analysis of fractured surfaces by SEM

Figure 37 showed the unaged and aged joints' fractured surfaces at higher levels of magnification. Note that, in these figures, the colour differences showed differences in electrical conductivity of the materials. A lack of conductivity was indicated by white due to a build-up of electrical charge that could not be transmitted to ground (Postek & Vladár, 2015). The epoxy used is not electrically conductive, and a thin layer of graphite had to be added to increase voltage absorption and reduce charge build up. In some cases, images were difficult to produce because even the samples themselves were not conductive.

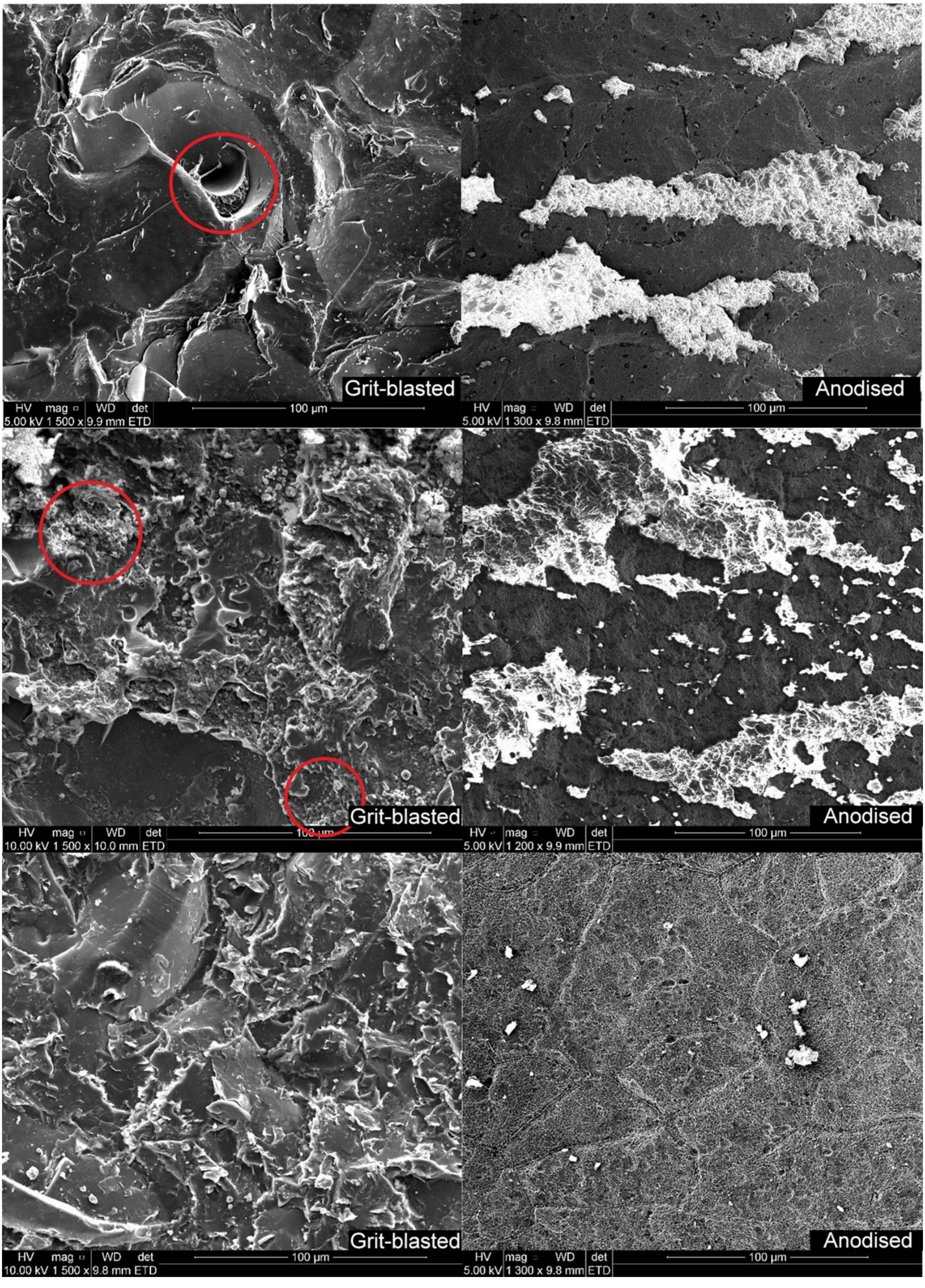

Figure 37: From top-down fractured surfaces of joints at 0 hours, 300 hours and 600 hours aged, respectively.

Figure 37 showed the fractured unaged anodised surface at 1300× magnification on the right, with what appears to be epoxy still adhered to the crevices in the surface shown in white. The grit-blasted surface at 1500× magnification did not show the same amount of epoxy on the surface, but some epoxy could be seen in scattered pockets and was circled in red for emphasis. Note the bubbles that formed within the epoxy; these bubbles were most likely the epoxy off-gassing as it cured, and because as the epoxy was mixed, air bubbles were incorporated in the mixture (Yin *et al.*, 2018). These bubbles were present in the grit-blasted and anodised joints for all ageing conditions.

The 300 hours-aged grit-blasted surface at 1500× magnification, shown in Figure 37, with nodules on the surface; two of these clusters were circled in red. These nodules could be indicative of oxidation from saltwater penetration into the bond that hydrate the aluminium oxide surface to create aluminium hydroxide (da Silva *et al.*, 2018; Goushegir *et al.*, 2020). To support this claim examples of hydroxide formation on aluminium from literature were given unmodified in Figure 38 and Figure 39.

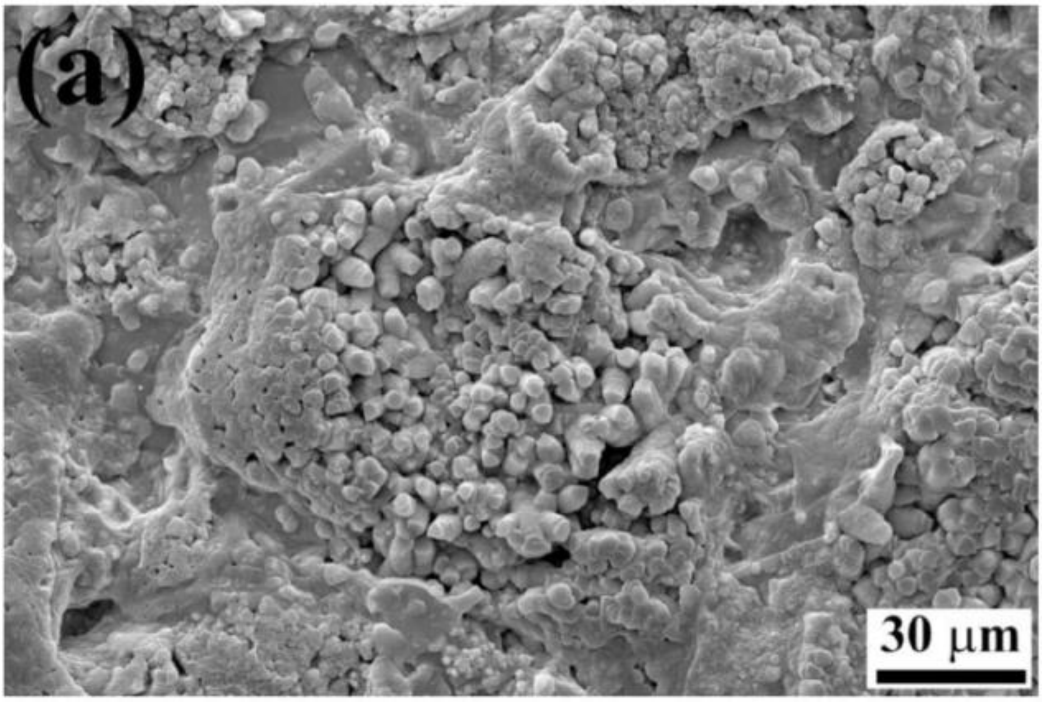

Figure 38: Example 1 of aluminium hydroxide formation (Goushegir et al., 2020)

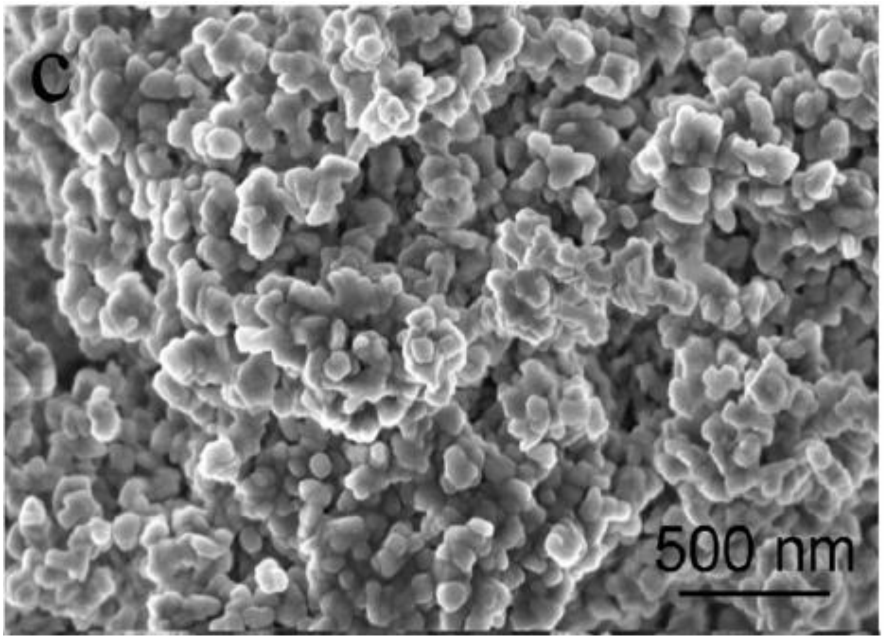

Figure 39: Example 2 of aluminium hydroxide formation (Kazantsev et al., 2018)

These same structures were found on grit blasted samples from this study as seen across Figure 40 and in the absence of EDS analysis gave high confidence that the grit blasted surfaces did have moisture ingress which led to the hydration of the aluminium oxide.

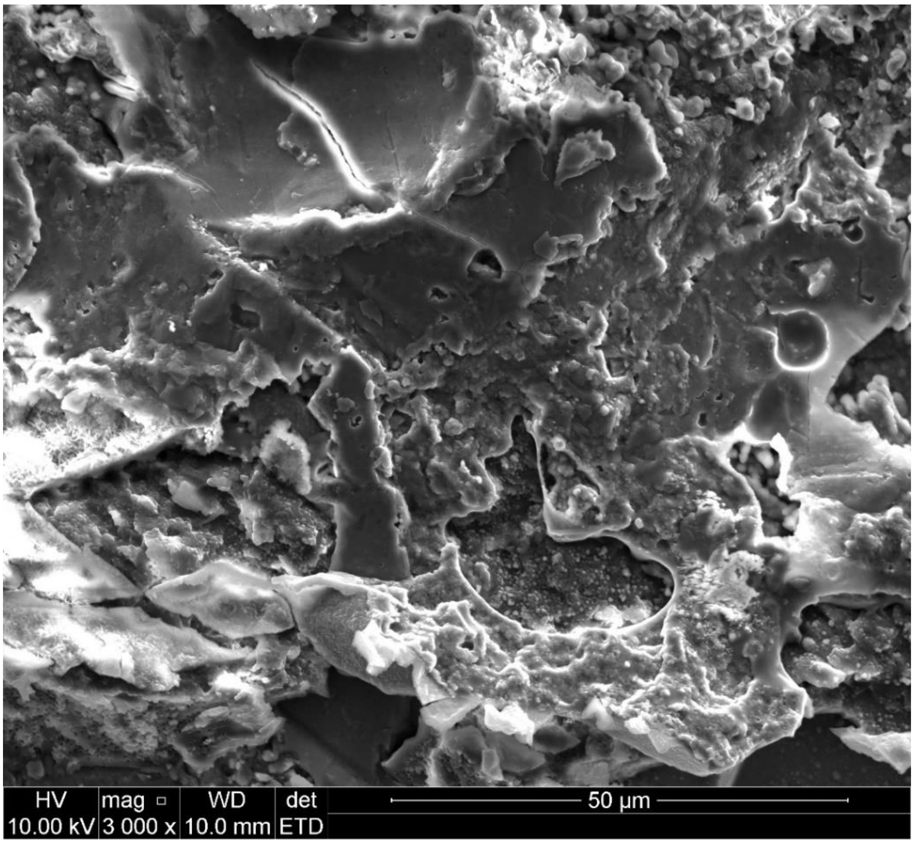

Figure 40 Grit blasted fracture surface after 300 hours of ageing

The anodised surface was like the unaged surface and showed epoxy still attached, shown in white, with no signs of oxidation at 1200× magnification. The lack of oxidation being due to the phosphate incorporated in the aluminium oxide layer that formed during anodising (da Silva *et al.*, 2018:170).

Figure 37 shows the fractured surface of the 600 hours-aged, anodised joint at 1300× magnification, with a marked decrease in the epoxy still adhered to the surface. This corresponded well to the observed decrease in lap shear strength but only served as an example of how the surface might look. This was because, as with all previous SEM images, they only showed a tiny part of the surface, and different structures can be present. This was shown again by looking at the grit-blasted surface at 1500× magnification, which looked unchanged by the ageing.

Figure 41 shows the 300 hours-aged joints at 6000× and 5000× magnification. An excellent example of epoxy interlocking was seen on the grit-blasted surface. The anodised surface also showed excellent interlocking within the crevices and pores with no signs of oxidation in either the grit-blasted or anodised joints.

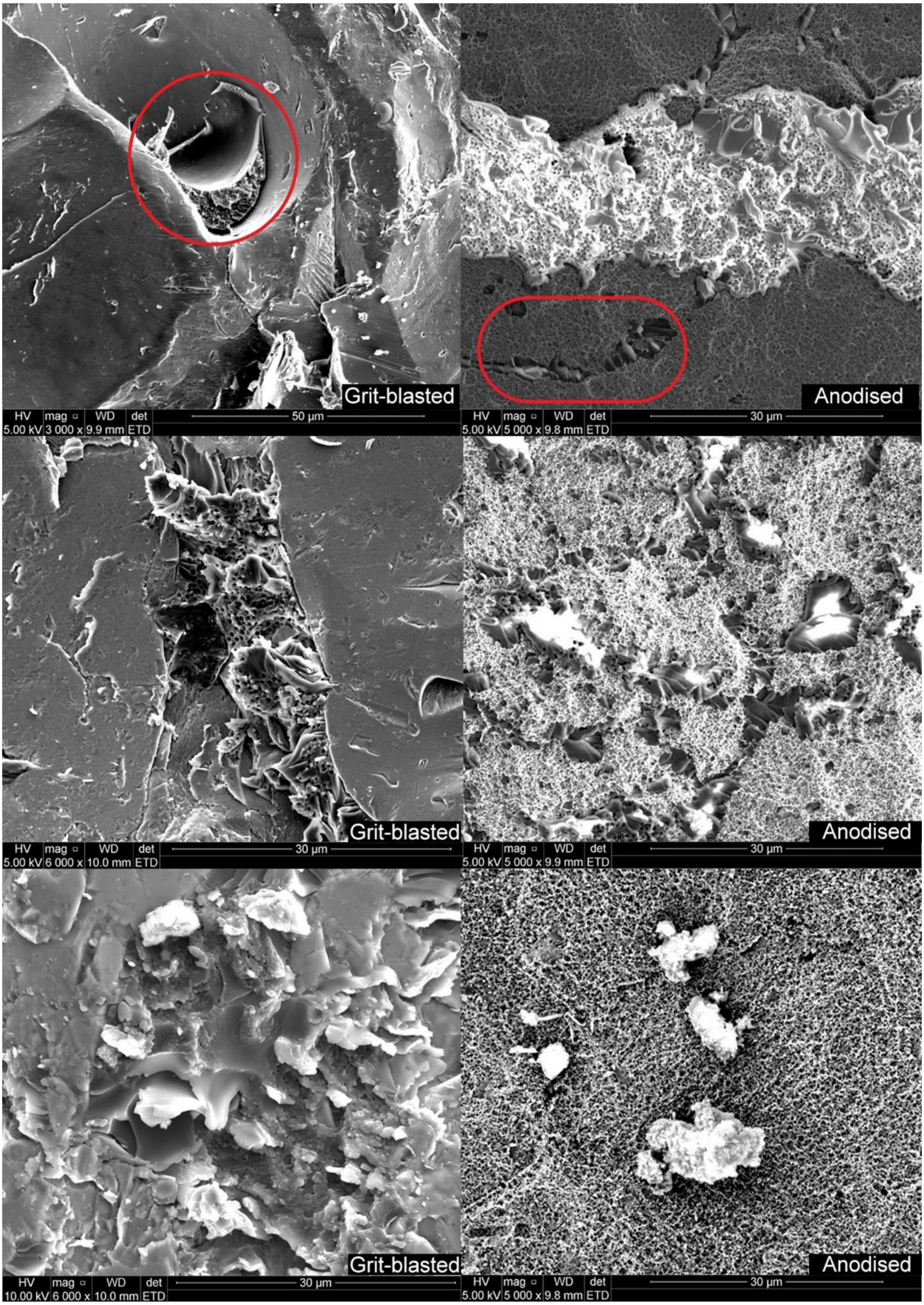

Figure 41: From top-down fractured surfaces of joints at 0 hours, 300 hours and 600 hours aged, respectively.

Figure 41 showed oxidation on the grit-blasted fracture at 6000× magnification, after

600 hours of ageing. The oxidation was less prevalent but can be seen as rounded structures in the image as was also found by Goushegir *et al. (2020)*. There seems to be no further degradation of the anodised surface when compared to the 300 hours aged samples.

A close-up of the red oval on the anodised side of Figure 41 is shown in Figure 42 to better illustrate the epoxy within the crevice.

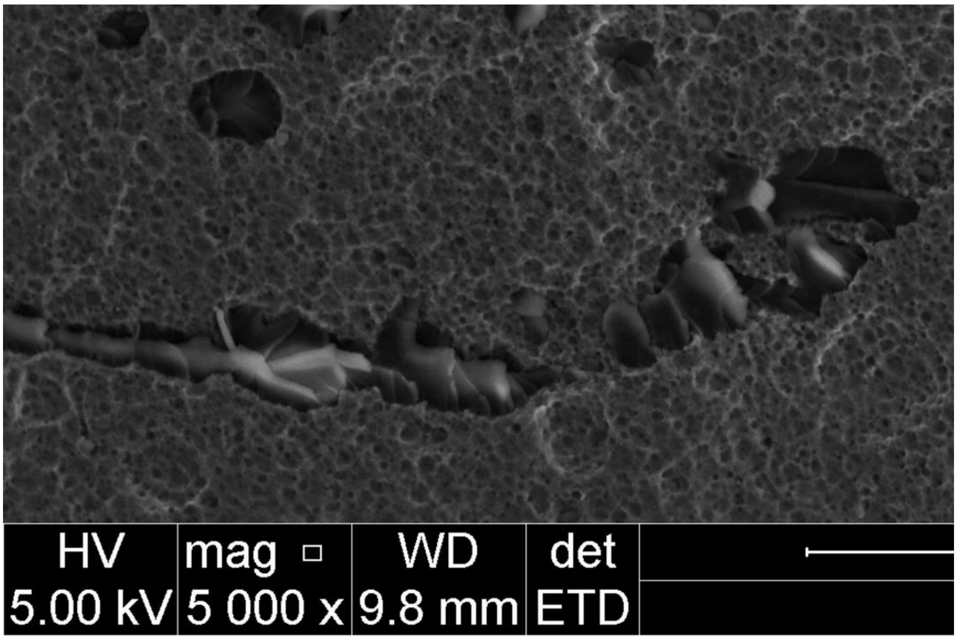

Figure 42: Close-up of red oval in Figure 44.

In summary, the SEM images showed a clear difference in the microstructures seen on the surfaces of the grit-blasted and anodised joints. The grit-blasted joints have a much smoother surface finish with no micropores, whilst the anodised surfaces are rougher and show micropores. Epoxy was seen in these micropores and crevices on the anodised surface but was much less prevalent on the grit-blasted surfaces. After ageing, the grit-blasted joints showed moisture ingress in the form of rounded structures on the surface, whilst the anodised joints showed no such structures.

5.8. Verification

ASTM D1002 was used as the base standard for testing in this study and recommends using 1.62 mm-thick, 101.6 mm × 25.4 mm aluminium coupons that have an adhesive overlap of 12.7 mm. Given that a 2 mm thick aluminium flat bar was used in this study, as it is readily available and much easier to cut into lengths, the standard ASTM D1002 method for testing the lap shear strength of aluminium joints could not be fully used. The coupons used in this study were cut to approximately 102 mm and came off-the-shelf with a width of 25 mm. Even though there is a slight difference in the coupon geometry, it allowed for a greater amount of data points and thus allowed more meaningful conclusions to be made. The adhesive overlap in this study was set to 25 mm because, as mentioned above, the thickness of the aluminium was more than the standard prescribes. Variations on the ASTM-D1002 standard, such as those done in this study, have been reported in the literature (Safari *et al.*, 2020).

To further verify that the changes made to the standard did not have a significant effect on results, a set of tests was done with an overlap of 12.7 mm, as per ASTM D1002, and that data is given below in Table 11. The samples made for this test were pretreated with the PAA method.

Table 11 Comparison between 25.4 mm and 12.7 mm overlap shear strengths unaged.

	Overlap	
	25.4 mm	12.7 mm
Average shear strength (MPa)	13.12	14.85
95% confidence lower limit (MPa)	12.81	13.84
99% confidence lower limit (MPa)	12.67	13.32
Standard deviation (MPa)	0.87	2.76

There is a slight increase in lap shear strength when a 12.7 mm overlap is used, and the difference may be attributed to a slight decrease in the moment that forms during a lap shear test due to the smaller overlap area. To further validate the claim, Welch's test was applied to these two datasets, and it proved that there was no significant difference in the means. These results are summarised in Table 12 below.

Table 12 Welch's test for 25.4mm vs. 12.7mm overlap

25.4 mm vs. 12.7 mm overlap	
Alpha	0.05
F-stat	1.31
df1	1
df2	12.31
p-value	0.27
sig	no

The tests were done on an MTS Landmark Servohydraulic System that was calibrated on the 10th of March, 2021, by SPS Calibration Services Pty Ltd. The calibration certificate can be found in Appendix A.

.

5.9. Validation

Results from the literature are comparable to results obtained in this study; some values are given here. Del Real *et al.* (2012) reported lap shear strengths of 15 MPa for abraded joints and 18 MPa for P2-treated joints. Harris and Beevers (1999) reported a lap shear strength of 3.20 MPa for grit-blasted joints. Safari *et al.* (2020) reported lap shear strengths between 3 MPa and 14.85 MPa for grit-blasted joints for two different epoxies. Ataberk (2020) reported lap shear strengths between 9 MPa and 15 MPa for PAA-treated joints.

6. Conclusions

The comparative performance of aluminium 6063-T6 bonded with SpaBond 345 epoxy after grit blasting and phosphoric acid anodising was studied. Lap shear tests performed on the unaged joints showed that anodised joints fail in a mixed mode of adhesive and cohesive failure, and that grit-blasted joints experience more adhesive failure. Aged, anodised joints were able to retain 91% and 74% strength after 300 and 600 hour ageing, respectively, whilst grit-blasted joints retained 74% and 88% strength after 300 and 600 hour ageing, respectively.

Due to the great number of samples that were tested, statistical analysis could be applied and proved that there are significant differences between surface pretreatments as well as the amount of time samples were aged for. This observation was consistent down to batch level where the difference in batch means for PAA samples were less than the grit blasted samples. Greater standard deviations and standard errors for grit blasted results indicated that grit blasted joints do not provide results that are consistent and repeatable as anodised joints. Anodised data points showed a tighter spread around the mean for all ageing conditions. These claims were further supported by the qualitative analysis of the surfaces.

Optical image analysis showed that apparent moisture ingress was more prevalent on grit-blasted joints than anodised joints. This qualitative observation was supported by the quantitative data already shown. It also showed a greater number of cohesive and mixed failures on anodised joints compared to grit-blasted joints which increasingly fractured in adhesion as the ageing time increased.

SEM analysis showed mechanical interlocking for both grit-blasted and anodised joints, but to a greater degree in anodised joints. Signs of aluminium oxidation were found in both the grit-blasted and anodised joints, but more so in the grit-blasted joint with complete oxidation and infiltration of moisture as indicated by the formation of aluminium hydroxide.

It was found that SpaBond 345 is suitable for adhering pretreated aluminium especially if anodised. If joints are not exposed to moisture for prolonged periods then grit blasting can also be considered at a reduction in lap shear strength.

All results confirmed the findings in the literature that indicate grit blasted joints may have comparative shear strength to anodised joints, but that have a greater tendency to degrade when aged.

7. Recommendations and further study

This study served well as a pilot for a breadth of further research. Given that it is a pilot project, it had various shortcomings that should be addressed in subsequent studies. These include but are not limited to the points that follow in this section.

An investigation should be done to determine the effect of accelerated ageing on the bulk adhesive. Even though differences in strength and variances were noted after ageing the bonds, the ageing process should ideally be extended to determine the point at which PAA samples break down in the same manner that the grit blasted samples in this study did. Along with this, a fatigue study should be done on these bonds, both unaged and after ageing because lap shear tests cannot fully characterize the behaviour of joints as discussed in the literature.

In addition, SpaBond 345 bulk samples should be aged and tested to determine the effect of water absorption. This is due to an effect called plasticization and as suggested by Sharp (2015) may increase the toughness of a given epoxy due to varying degrees of moisture absorption.

Given that anodising is commonly paired with various other surface pretreatments, as shown in the literature discussed, these interactions should be investigated. Some of these include the effect of sealing the anodised layer after it is created by boiling in water, dipping the anodised surface in a primer or epoxy to allow extended shelf-life, or using grit blasting in combination with the anodising. In addition, grit blasting should be further investigated to determine the effect that impingement angle, dwell time, and stand-off distance will have on the surface being blasted.

As noted, the lap shear test is a very effective method of quickly ascertaining the strength of a bond, but it does have drawbacks. Other testing methods, such as those mentioned in the literature review of this study, should be further examined.

Further EDS analysis should be done to confirm the exact surface composition of fractured samples before and after ageing to give a better understanding of the level of moisture ingress that occurs.

References

Abd-Elnaiem, A.M., Abbady, G., Ali, D. & Asafa, T.B. 2019. Influence of anodizing voltage and electrolyte concentration on Al-1 wt % Si thin films anodized in H2SO4. *Materials Research Express*,

Araoyinbo, A.O., Noor, A.F.M., Sreekantan, S. & Aziz, A. 2010. VOLTAGE EFFECT ON ELECTROCHEMICAL ANODIZATION OF ALUMINUM AT AMBIENT TEMPERATURE. *International Journal of Mechanical and Materials Engineering*, 5(1):53-58.

Arenas, J.M., Narbón, J.J. & Alía, C. 2010. Optimum adhesive thickness in structural adhesives joints using stastical teckniques based on Weibull distribution. *International Journal of Adhesion and Adhesives*, 30(3):160-165.

Aspenes, G., Høiland, S., Barth, T., Askvik, K.M., Kini, R.A. & Larsen, R. 2008. Petroleum hydrate deposition mechanisms: The influence of pipeline wettability. In: Vancouver.

Ataberk, N. 2020. The effect of Cu nanoparticle adding on to epoxy-based adhesive and adhesion properties. *Scientific Reports*, 10,

Barrett, R.T. 1990. *Fastener Design Manual*.

Board, N.T.S. 1989. *Aircraft Accident Report--Aloha Airlines, Flight 243,*. Washington D.C.

Borrie, D., Al-Saadi, S., Zhao, X.-L., Raman, R.K.S. & Bai, Y. 2021. Bonded CFRP/Steel Systems, Remedies of Bond Degradation and Behaviour of CFRP Repaired Steel: An Overview. *Polymers*, 13(9):1533.

Boutar, Y., Naïmi, S., Mezlini, S. & Ben Sik Ali, M. 2016. Effect of surface treatment on the shear strength of aluminium adhesive single-lap joints for automotive applications. *International Journal of Adhesion & Adhesives*, 67:38-43.

Brewis, D.M., Critchlow, G.W. & Curtis, C.A. 1999. Cryoblasting as a pretreatment to enhance adhesion to aluminium alloys: an initial study. *International Journal of Adhesion & Adhesives*, 19:253-256.

Broad, R., French, J. & Sauer, J. 1999. New, effective, ecological surface pretreatment for higly durable adhesively bonded metal joints. *Internation Journal of Adhesion & Adhesives*, 19:193-198.

Broughton, B. 2000. *Measurement Good Practice Guide No. 28: Durability Performance of Adhesive Joints*. Teddington.

Cartwright, T. 2005. *Non-standard Anodisation Processes for the Pretreatment of Structurally Bonded Aluminium Alloys*.

Corporation, A. 2015. *Anodize Coatings*. Syracuse.

Coulon, J.-F. & Maillard, H. 2010. Epoxy based composite surface analysis. A plasma treatment for wettability evolution. *The European Physical Journal Applied Physics*, 49(1),

Council, A.A. Anodizing and the Environment. https://www.anodizing.org/page/anodizing-environmental-advantages

Council, N.R. 1996. *Accelerated Aging of Materials and Structures: The Effects of Long-Term Elevated-Temperature Exposure*. Washington, DC: National Academies Press.

Critchlow, G.W. & Brewis, D.M. 1995. Influence of surface macroroughness on the durability of epoxide-aluminium joints. *International Journal of Adhesion and Adhesives*, 15:173-176.

Critchlow, G.W. & Brewis, D.M. 1996. Review of surface pretreatmens for aluminium alloys. *International Journal of Adhesion and Adhesives*:255-275.

Critchlow, G.W., Yendall, K.A., Bahrani, D., Quinn, A. & Andrews, F. 2006. Strategies for the replacement of chromic acid anodising for the structural bonding of aluminium alloys. *International Journal of Adhesion & Adhesives*, 26(6):419-453.

da Silva, L.F.M., Ochsner, A. & Adams, R.D. 2018. *Handbook of Adhesion Technology*. Springer International Publishing AG.

da Silva, L.F.M., Rodrigues , T.N.S.S., Figueiredo, M.A.V., de Moura, M.F.S.F. & Chousal, J.A.G. 2006. Effect of Adhesive Type and Thickness on the Lap Shear Strength. *The Journal of Adhesion*, 82(11):1091-1115.

da Silva, L.F.M., Carbas, R.J.C., Critchlow, G.W., Figueiredo, M.A.V. & Brown, K. 2009. Effect of material, geometry, surface treatment and environment on the shear strength of single lap joints. *International Journal of Adhesion & Adhesives*, 29:621-632.

Del Real, J.C., De Santayana, M.C., Abenojar, J. & Martinez, M.A. 2006. Adhesive bonding of aluminium with structural acrylic adhesives: durability in wet environments. *Journal of Adhesion Science and Technology*, 20(16):1801-1818.

Del Real, J.C., Cano de Santayana, M., Abejonar, J. & Martinez, M.A. 2012. Adhesive bonding of aluminium with structural acrylic adhesives: durability in wet environments. *Journal of Adhesion Science and Technology*, 20(16):1801-1818.

Delacre, M., Lakens, D. & Leys, C. 2017. Why Psychologists Should by Default Use Welch's t-test Instead of Student's t-test. *International Review of Social Psychology*, 30(1):92-101.

Demko, S.M., Hedman, D. & Locks, W. 1999. *National Transportation Safety Board-NYC99LA102*. New Milford.

Digby, R.P. & Packham, D.E. 1995. Pretreatment of aluminium: topography, surface chemistry and adhesive bodn durability. *Int. J. Adhesion and Adhesives*, 15(2), Ding, Z., Smith, B.A., Hebert, R.R., Zhang, W. & Jaworowski, M.R. 2018. Morphology perspective on chromic acid anodizing replacement by thin film. *Surface & Coatings Technology*, 350:31-39.

Duncan, B. 2010. *Advances in Structural Adhesive Bonding*. Woodhead Publishing.

Ebnesajjad, S. & Landrock, A.H. 2015. *Introduction and Adhesion Theories*. William Andrew Applied Science Publishers.

Erich, M., Nair, G. & Barkhimer, J. 2015. *Effect of Time Delay Between Etching and Adhesive Bonding ("Outlife" Time) on Lap-Shear Strength of Aluminium Alloys Using Environmentally-Friendly P2 Etch*. San Luis Obispo.

Ghara, T., Paul, S. & Bandyopadhyay, P.P. 2021. Effect of Grit Blasting Parameters on Surface and Near-Surface Properties of Different Metal Alloys. *Journal of Thermal Spray Technology*, 30:251-269.

Goushegir, S.M., Scharnagl, N., dos Santos, J.F. & Amancio-Filho, S.T. 2020. Durability of Metal-Composite Friction Spot Joints under Environmental Conditions. *Materials*,

Harris, A.F. & Beevers, A. 1999. The effects of grit-blasting on surface properties for adhesion. *International Journal of Adhesion & Adhesives*, 19:445-452.

Heinzmann, C., Weder, C. & de Espinosa, L.M. 2015. Supramolecular polymer adhesives: advanced materials inspired by nature. *Chemical Society Reviews*, 45(2),

Higgins, B.G. 1988. Surface tension of curing epoxy. *Journal of Polymer Science Polymer Chemistry Edition*, 26(7),

Hutchinson, A. 1993. *Environmental Durability Test Procedures*. Oxfordshire.

Information, N.C.f.B. 2023. *PubChem Compound Summary for CID 6278, 1,1,1-Trichloroethane* https://pubchem.ncbi.nlm.nih.gov/compound/1_1_1-Trichloroethane

Jarque, C.M. & Bera, A.K. 1987. A Test for Normality of Observations and Regression Residuals. *International Statistical Review*, 55(2):163-172.

K, S. & Alagar, M. 2014. Thermo-mechanical and dielectric properties of graphene reinforced caprolactam cardanol based benzoxazine-epoxy nanocomposites. *RSC Advances*, 5(13),

Kang, G. & Choi, W. 2021. A Study on the Effects of Surface Energy and Topography on the Adhesive Bonding of Aluminum Alloy. *Korean Journal of Metals and Materials*, 59(8):567-574.

Kazantsev, S.O., Lozhkomoev, A.S., Glazkova, E.A., Gotman, I., Gutmanas, E.Y., Lemer, M.I. & Psakhie, S.G. 2018. Preparation of aluminum hydroxide and oxide nanostructures with controllable morphology by wet oxidation of AlN/Al nanoparticles. *Materials Research Bulletin*, 104:97-103.

Kuczmaszewski, J. & Zawada-Michałowska, M. 2020. Quality of Samples in Adhesive Joint Testing. *Advances in Science and Technology Research Journal*, 14(3):182-191.

Kudelka, J. 2011. *Anodizing for Bonding Applications in Aerospace* https://www.pfonline.com/articles/developing-standardized-testing-for-trivalent-chromium-thickness-a-progress-report

Labor, U.S.D.o. 2006. *Health Effects of Hexavalent Chromium*.

Lee, S., Kim, D., Kim, Y., Jung, U. & Chung, W. 2016. Effect of Aluminium Anodizing in Phosphoric Acid Electrolyte on Adhesion Strength and Thermal Performance. *Metals and Materials International*, 22(1):20-25.

Legdin, E. 2017. *Joining of metal and fiber composites*. Stockholm.

Li, J., Huang, M., Xiang, Y., Bi, R., Tu, C. & Wang, B. 2019. Surface Treatment for Improving Durability of Aluminum-Lithium Adhesive-Bonded Joints under Hot-Humid Exposure. *Coatings*,

Li, T., Heinzer, M.J., Redline, E.M., Zuo, F., Bates, F.S. & Francis, L.F. 2014. Microstructure and performance of block copolymer modified epoxy coatings. *Progress in Organic Coatings*, 77:1145-1154.

Mart, A.M. 2023. *MAC AFRIC Bench Type Sand Blast Cabinet* https://www.adendorff.co.za/product/mac-afric-bench-type-sand-blast-cabinet/

Matta, A., Sedlacek, T., Kadleckova, M. & Lengalova, A. 2022. The Effect of Surface Substrate Treatments on the Bonding Strength of Aluminium Inserts with Glass-Reinforced Poly(phenylene) Sulphide. *Materials*, 15,

Mattson, C. They Physics of Adhesion. http://ffden-2.phys.uaf.edu/webproj/212_spring_2014/Connor_Mattson/connor_mattson/physics.html

McDonald, J.H. 2009. Student's T-Test. In. *Handbook of Biological Statistics*. Maryland: Sparky House Publishing. p 120.

Melhem, G.N. 2018. Aerospace Fasteners: Use in Structural Applications. In: Totten, G.E., Tiryakioğlu, M. & Kessler, O., eds. *Encyclopedia of Aluminum and Its Alloys*. Boca Raton: CRC Press. pp. 30-45.

Min, J., Wan, H., Carlson, B.E., Lin, J. & Sun, C. 2020. Application of laser ablation in adhesive bonding of metallic materials: A review. *Optics and Laser Technology*, 128,

Momm, G.G., Ilcewicz, L., Ashforth, C. & Fleming, D. 2021. *Bond-related Aircraft Accidents/Incidents: A Review*. New Jersey.

Narbon, J.J., Moreno-Díaz, C. & Arenas, J.A. 2018. Influence of surface treatment on the surface energy of an aluminium substrate. *Colloids and Surfaces A*:323-329.

Niknahad, M., Moradian, S. & Mirabedini, S.M. 2010. The adhesion properties and corrosion performance of differently pretreated epoxy coatings on an aluminium alloy. *Corrosion Science*, 52:1948-1957.

Orazi, L., Montanari, F., Campana, G., Tomesani, L. & Cuccolini, G. 2015. CNC Paths Optimization in Laser Texturing of Free Form Surfaces. In.: Science Direct.

Ostapiuk, M., Surowska, B. & Bieniaś, J. 2014. Interface analysis of fiber metal laminates. *Composite Interfaces*, 21(4):309-318.

Ozenc, M. & Sekercioglu, T. 2013. *Effect of surface pre-treatment and temperature on the adhesive strength of hybrid aluminium joints*. Kinikli.

Petersson, L., Meier, P., Kornmann, X. & Hillborg, H. 2011. Effect of surface cleanliness of aluminium substrates on silicone rubber adhesion. *Journal of Physics D: Applied Physics*, 44(3),

Pires, I., Quintino, L. & Miranda, M. 2005. Performance of 2024-T3 Aluminium Adhesive Bonded Joints. *Materials and Manufacturing Processes*, 20:175-185.

Possart, W., Bockenheimer, C. & Valeske, B. 2002. The state of metal surfaces after blasting treatment Part 1: Technical aluminium. *Surface and Interface Analysis*, 33:687-696.

Postek, M.T. & Vladár, A.E. 2015. Does your SEM really tell the truth? How would you know? Part 4: Charging and its mitigation. In: Monterey.

PriceWalgren. 2020. *Anodizing Equipment / Aluminium Finishing*.

Prolongo, S.G. & Ureña, A. 2009. Effect of surface pre-treatment on the adhesive strength of epoxu-aluminium joints. *International Journal of Adhesion & Adhesives*, 29:23-31.

Rechner, R., Jansen, I. & Beyer, E. 2010. Influence on the strength and aging resistance of aluminium joints by laser pre-treatment and surface modification. *International Journal of Adhesion & Adhesives*, 30:595-601.

Reitz, V., Meinhard, D., Ruck, S., Riegel, H. & Knoblauch, V. 2017. A comparison of IR- and UV-laser pretreatment to increase the bonding strength of adhesively joined aluminum/CFRP components. *Composites: Part A*, 96:18-27.

Risbrudt, C.D., Ross, R.J., Blankenburg, J.J. & Nelson, C.A. 2007. Forest Products Laboratory Supporting the Nation's Armed Forces with Valuable Wood Research for 90 Years. *Forest Products Journal*, 57(1):11.

Romoli, L., Lutey, A.H. & Moroni, F. 2018. Pulsed Laser Pre-Treatment of Aluminium Adhesive Bonded Joints: Process Parameter Selection for Improved Fatigue Resistance. *Lasers in Engineering*, 41(4-6):317-331.

Rotella, G., Alfano, M., Schiefer, T. & Jansen, I. 2016. Evaluation of mechanical and laser surface pre-treatments on the strength of adhesive bonded steel joints for the automotive industry. *Journal of Adhesion Science and Technology*, 30(7):747-758.

Rudawska, A., Stančeková, D., Cubonova, N., Vitenko, T., Müller, M. & Valášek, P. 2017. Adhesive properties and adhesive joint strength of graphite/epoxy composites. *Journal of Physics Conference Series*, 842(1),

Ryan, V. 2018. Revision Cards - Anodising. https://technologystudent.com/joints_flsh/revcard_metal1.html

Safari, A., Farahani, M. & Ghabezi, P. 2020. Experimental study on the influence of different surface treatment processes and adhesive type on the aluminum adhesive-bonde joint strength. *Mechanics Based Design of Structures and Machines*,

Saint-Gobain. 2020. *Accelerating Automative Assembly with Norbond® Attachment Tapes* https://www.tapesolutions.saint-gobain.com/na/technical-articles/accelerating-automotive-assembly-norbond-attachment-tapes#

Saleema, N., Sarkar, D.K., Paynter, R.W., Gallant, D. & Eskandarian, M. 2012. A simple surface treatment and characterization of AA 6061 aluminum alloy surface for adhesive bonding applications. *Applied Surface Science*, 261:742-748.

Sharp, N. 2015. *Effects of moisture on the properties of epoxies and carbon-epoxy composite laminates.* Purdue University.

Slătineanu, L., Potârniche, Ş., Coteaţă, M., Grigoraş, I., Gherman, L. & Negoescu, F. 2011. Surface roughness at alumnium parts sand blasting. *Proceedings in Manufacturing Systems*, 6(2):69-74.

Sorrentino, L., Polini, W., Bellini, C. & Parodo, G. 2018. Surface treatment of CFRP: influence on single lap joint performances. *Internation Journal of Adhesion and Adhesives*, 85:225-233.

Sulka, G.D. & Parkola, K.G. 2006. Anodising potential influence on well-ordered nanostructures formed by anodisation of aluminium in sulphuric acid. *Thin Solid Films*, 515:338-345.

Sulka, G.D. & Parkola, K.G. 2007. Temperature influence on well-ordered nanopore structures grown by anodization of aluminium in sulphuric acid. *Electrochimica Acta*, 52:1880-1888.

Technology, M.T. 2016. *ASTM.D1002.03 - METAL TO METAL LAP SHEAR SPECIMEN FABRICATION FIXTURE (SS)* https://www.youtube.com/watch?v=at3xo6SVWes

TWI. 2002. Adhesive Toolkit. http://www.adhesivestoolkit.com/Docs/test/MECHANICAL%20TEST%20METHOD%201%20-%20Shear%20Tests.xtp#_Toc109014547 Date of access: April.

Udatha, P., Babu, Y.N., Satyadev, M. & Bhagavathi, L.R. 2019. Effect of natural fibers reinforcement on lap-shear strength of adhesive bonded joints. *Materials Today: Proceedings*:541-544.

Xu, Y., Li, H., Shen, Y., Liu, S., Wang, W. & Tao, J. 2016. Improvement of adhesion performance between aluminium sheet and epoxy based on anodizing technique. *International Journal of Adhesion & Adhesives*, 70:74-80.

Yin, Y.-B., Yang, Q.-S., Wang, S.-L., Gao, H.-D., He, Y.-W. & Li, X.-L. 2018. Formation of CO2 bubbles in epoxy resin coatings: A DFT study. *Journal of Molecular Graphics Modelling*, 86:192-198.

Zhang, Z., Shan, J.-G., Tan, X.-H. & Zhang, J. 2017. Effect of anodizing pretreatment on laser joining CFRP to aluminum alloy A6061. *International Journal of Adhesion & Adhesives*, 70:142-151.

Appendix A

Designs

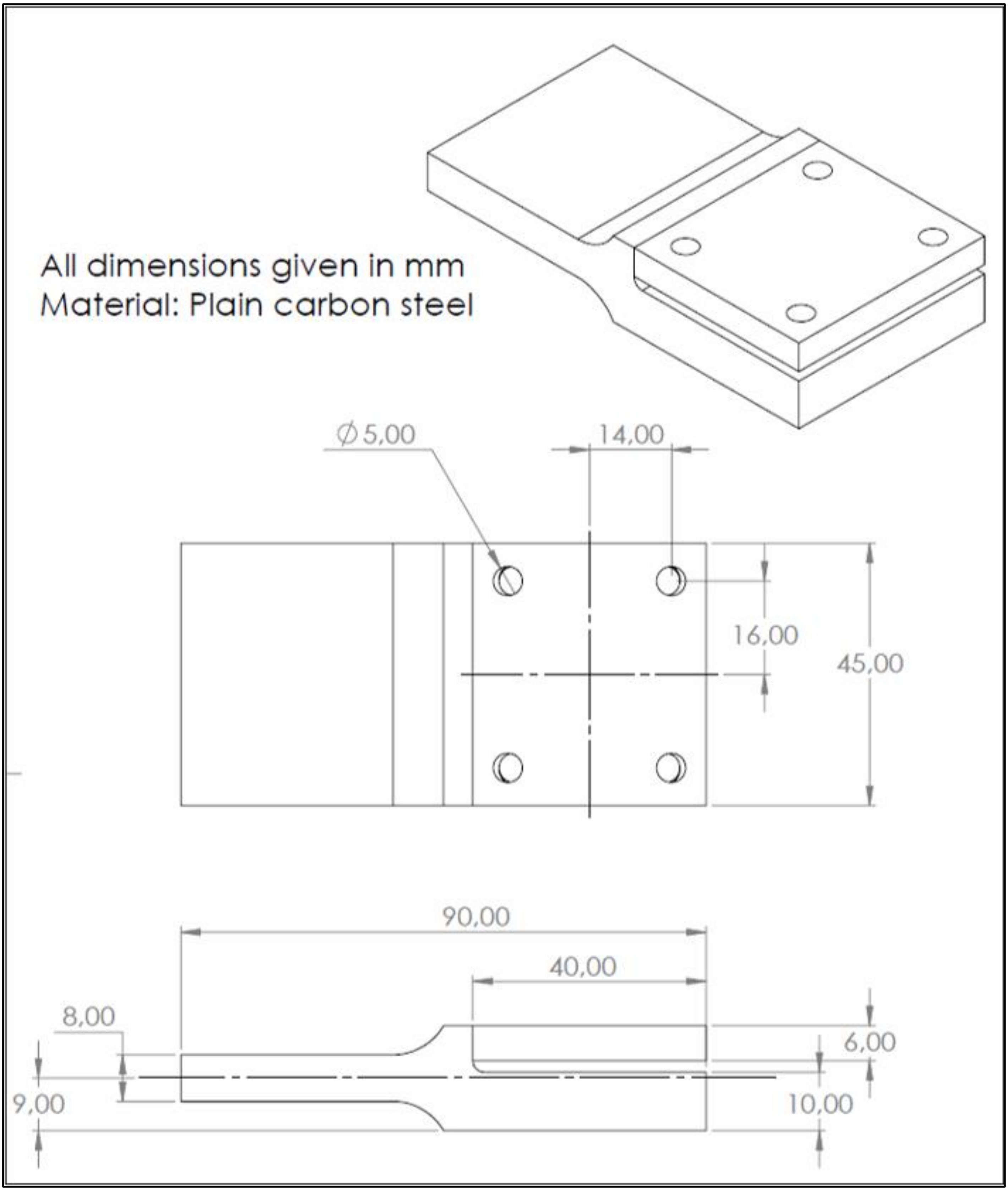

Figure 43: Testing alignment jig detail drawing.

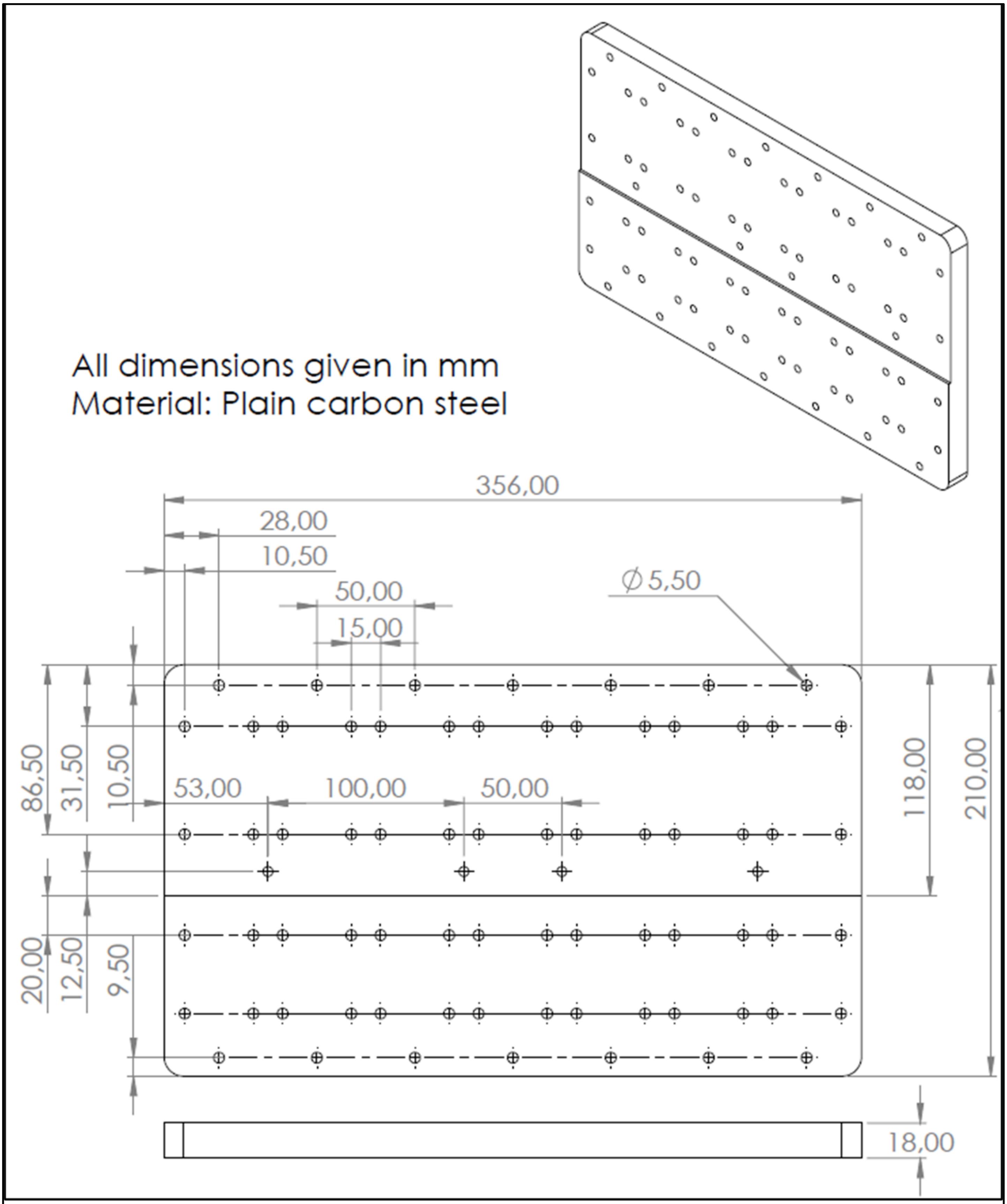

Figure 49 Adhesion alignment jig base detail drawing

Figure 44: Adhesion alignment jig base detail drawing.

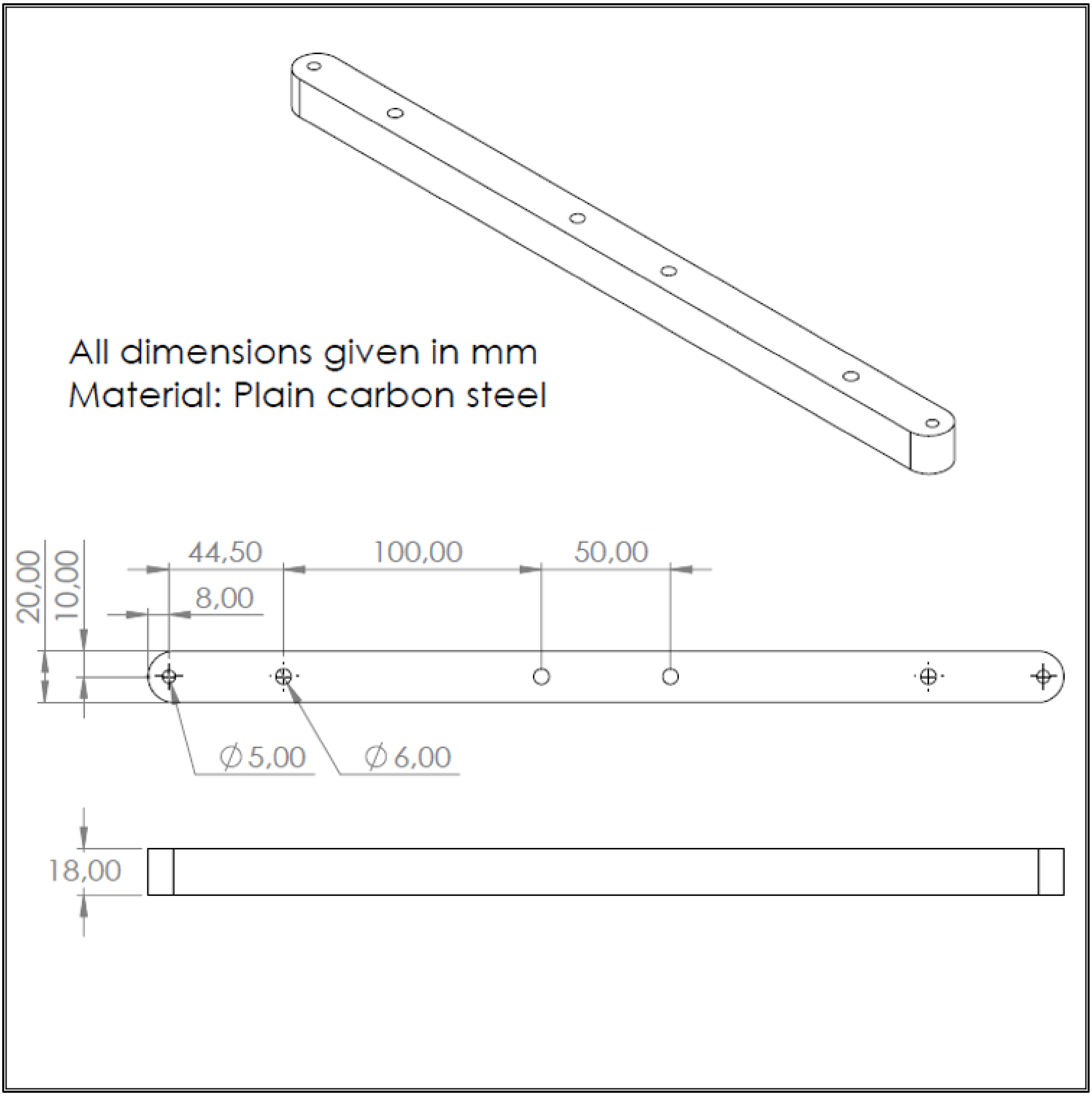

Figure 45: Adhesion alignment jig pressure plate detail drawing.

Calibration certificate

ON SITE CALIBRATION CERTIFICATE
OF A UNIVERSAL TESTING MACHINE
SANAS ACCREDITED LABORATORY FOR FORCE - NO: 816

CALIBRATION CERTIFICATE NUMBER: NHQ-88755 A

This certificate is a correct record of the measurements made by standards traceable to National Measurement Institute South Africa (NMISA) and International Standards.

Company:	NORTH WEST UNIVERSITY - POTCHEFSTROOM
Contact Person:	MR. SAREL NAUDE
Physical Address:	HOFFMAN STREET, POTCHEFSTROOM
Location of Calibration:	LABORATORY BUILDING G15
Date of Calibration:	2021/03/10
Calibrated by:	F. CLASSEN / S. CILLIERS
Item Calibrated:	DYNAMIC TESTING MACHINE
Manufacturer:	MTS
Model Number:	LANDMARK
Universal Tester Serial Number:	10359599
Load Cell / Transducer Serial Number:	400803
Capacity of Machine:	100 kN
Resolution of Machine:	0.01 kN
Range Calibrated:	0 kN to 90 kN
Standard Used:	100kN LOAD CELL (115696 / 3152)
Traceability Number:	SHQ-86570 H
Procedure Followed:	FP1301

The accuracy's of the standards used are, by way of regular inter-comparison, traceable to National Standards, with the limitations of the services available. The measurement results in the certificate are correct at the time of calibration. Subsequently the accuracy will depend on such factors as the care exercised in handling as well as use of instruments, equipment and the frequency of use. No long term stability checks were carried out. This certificate automatically expires if the instrument is repaired or if the seal is broken. It is recommended that re-calibration be undertaken at an interval that will ensure that the instrument remains within the desired limits. The measurement results relate only to this item calibrated.

*Page 1 of 3

www.spsrsa.co.za
info@spsrsa.co.za
SPS Calibration Services (Pty) Ltd | Reg no. 2016/547509/07 | VAT no. 4210273431
Cnr. Christopher and Commissioner Str, Boksburg East | +27 11 918 5000
Director: MJS Matthysen